

AD-A060 757 MARYLAND UNIV COLLEGE PARK DEPT OF PHYSICS AND ASTRONOMY F/G 17/2  
THE UNIVERSITY OF MARYLAND PROPOSAL TO DEVELOP DIGITAL DATA HAN--ETC.(U)  
MAY 78 D G CURRIE N00014-75-C-1176

UNCLASSIFIED

NL

1 OF 1

AD  
A060 757



AD A060757

DDC FILE COPY

FINAL REPORT

for

N 00014-75-C-1176

FOR THE UNIVERSITY OF MARYLAND PROPOSAL TO  
DEVELOP DIGITAL DATA HANDLING AND PROCESSING EQUIPMENT  
FOR LLL SENSORS IN THE PRE-DETECTION COMPENSATION AND MAAI SYSTEMS

12  
LEVEL II

by

Douglas G. Currie

Submitted to

THE OFFICE OF NAVAL RESEARCH

395-549  
DDC  
NOV 2 1978  
F

May 1978



This document has been approved  
for public release and sale; its  
distribution is unlimited.

UNIVERSITY OF MARYLAND  
DEPARTMENT OF PHYSICS AND ASTRONOMY  
COLLEGE PARK, MARYLAND

78 10 23 149  
~~78 07 06 008~~

9 FINAL REPORT

for

15 N 00014-75-C-1176

6 THE UNIVERSITY OF MARYLAND PROPOSAL TO  
DEVELOP DIGITAL DATA HANDLING AND PROCESSING EQUIPMENT  
FOR LLL SENSORS IN THE PRE-DETECTION COMPENSATION AND MAAI SYSTEMS

by

10 Douglas G. Currie

Submitted to

THE OFFICE OF NAVAL RESEARCH

11 May 1978

12 95p.

University of Maryland  
Department of Physics and Astronomy  
College Park, Maryland 20742

APPROVED FOR PUBLIC RELEASE; DISTRIBUTION UNLIMITED

219 638 78 07 06 008

Gew

## ABSTRACT

The University of Maryland has developed a specialized data system for the operational and the data recording requirements of the Multi-Aperture Amplitude Interferometer. The primary role of this data system is the operation of the University of Maryland Array Photometer. This array photometer is essentially an extremely sensitive low light level television, with special requirements on its various modes of operation. Thus we shall discuss its ability to take long integration pictures, scan rapidly, and partially scan an array. This procedure will increase the dynamic range by a factor as large as one hundred and will increase the frame rate up as high as several thousand frames per second. Several other special techniques which have been developed for the University of Maryland Array Photometer will be discussed and some of the results described.

ACCESSION for	
NTIS	White Section <input checked="" type="checkbox"/>
DDC	Buff Section <input type="checkbox"/>
UNANNOUNCED	
JUSTIFICATION	
BY DISTRIBUTION/AVAILABILITY SECT	
S. CHAL	
A	



## TABLE OF CONTENTS

ABSTRACT . . . . .	1
TABLE OF CONTENTS . . . . .	11
TABLE OF FIGURES . . . . .	iv
I. INTRODUCTION . . . . .	1
II. CIRCULATING SEMICONDUCTOR MEMORY . . . . .	2
A. Basic Memory Parameters . . . . .	2
B. Input - Output Structure . . . . .	4
C. Logical Functions . . . . .	5
D. Monitor Displays . . . . .	6
E. System Structure . . . . .	6
F. Current Status . . . . .	7
G. Next Generation . . . . .	8
III. SINGLE SCAN DATA RECORDING SYSTEM . . . . .	9
IV. FRAME ADDITION . . . . .	10
V. SINGLE PHOTOELECTRON DETECTION . . . . .	12
VI. SKELETON AND SCANNING PROCEDURE . . . . .	14
A. Basic Procedure . . . . .	14
B. Control Word Structure . . . . .	14
C. Subscanning Option . . . . .	14
D. Time Resolution . . . . .	17
VII. DEMONSTRATION OF PARTIAL SCANNING PERFORMANCE . . . . .	18
A. Data Recording Modes . . . . .	18
B. Unresolved Images . . . . .	18
C. Partial Frame Scan Using Satellite Images . . . . .	26
PROGRAM CONCLUSIONS . . . . .	31

TABLE OF CONTENTS  
(Continued)

APPENDIX I . . . . .	34
CSM CONTROL WORD FORMAT	
APPENDIX II . . . . .	36
SAMPLE SKELETON SEQUENCES	
APPENDIX III . . . . .	40
ON A PHOTON COUNTING ARRAY USING THE FAIRCHILD CCD201	
APPENDIX IV . . . . .	68
AN INTENSIFIED CHARGE COUPLED DEVICE FOR EXTREMELY LOW LIGHT LEVEL OPERATION	

## TABLE OF FIGURES

Figure 1 - UMAP System Used in the Direct Imaging Camera Mode . . . . .	6
Figure 2 - Linear Digital Display of M3 . . . . .	12
Figure 3 - Logarithmic Digital Display of M3 . . . . .	12
Figure 4 - Pulse Height Distribution for CCD Image of M25 . . . . .	13
Figure 5 - Discriminated Digital Display of M3 . . . . .	14
Figure 6 - Monitor Display of Dark Current . . . . .	20
Figure 7 - Monitor Display of Overexposed Point Source . . . . .	20
Figure 8 - Digital Display of Overexposed Point Source . . . . .	20
Figure 9 - Quarter Chip Scan Dark Current . . . . .	22
Figure 10 - Quarter Chip Scan of Overexposed Point Source . . . . .	23
Figure 11 - Dark Subtracted Point Under Quarter Scan . . . . .	23
Figure 12 - Tenth Chip Scan of Overexposed Point Source . . . . .	24
Figure 13 - Tenth Chip Scan Dark Current . . . . .	25
Figure 14 - Digital Tenth Chip Scan of Overexposed Point Source . . . . .	26
Figure 15 - DSCS II Monitor Display . . . . .	28
Figure 16 - DSCS II Under Digital "Square Root" Display . . . . .	28
Figure 17 - Monitor Image of Bright DSCS II . . . . .	29
Figure 18 - Digital Display of Bright DSCS II . . . . .	29
Figure 19 - Quarter Chip Scan of Bright DSCS II . . . . .	30
Figure 20 - Digital Quarter Chip Scan of Bright DSCS II . . . . .	30

## 1. INTRODUCTION

The University of Maryland has been developing a unique new detector system, the Multi-Aperture Amplitude Interferometer. This system will permit the diffraction limited image information to be obtained on telescopes from the earth. The Multi-Aperture Amplitude Interferometer (MAAI) requires the use of a specially developed array photomultiplier. This array photomultiplier must detect single photoelectrons, scan rapidly, and have a number of special features. Within the Amplitude Interferometry Program, we have developed the University of Maryland Array Photometer to provide this function.

Under this grant, we have developed special test procedures and special scanning procedures. The test procedures permit an increase in accuracy by several orders of magnitude. The special scanning procedures permit an increase in dynamic range of up to a factor of 100.



## II. CIRCULATING SEMICONDUCTOR MEMORY

In this section we provide a general description of the Circulating Semiconductor Memory (CSM). This specialized unit provides a variety of functions but primarily serves as a high-speed large-capacity memory and as a control system for the scanning of the Charge Coupled Device (CCD). This Circulating Semiconductor Memory has now been in operation, fully interfaced to the minicomputer system, for over two years. During this period, the Circulating Semiconductor Memory has performed very well. It has been used for both studies of direct imaging using the University of Maryland Array Photometer and for development of the Multi-Aperture Amplitude Interferometer. We will now consider some of the structure of this unit.

### A. Basic Memory Parameters

The basic parameters of the memory portion of the Circulating Semiconductor Memory consists of

#### 1. Five Parallel Storage Tracks

The memory has five storage tracks. Each of these tracks may be accessed independently by the NOVA minicomputer system both in order to remove data and in order to enter both chip scan control sequences\* and data. Each of the tracks are also accessed independently by inputs at high speed from the video data processor which converts the data from the two scanning ICCD's into 5 data streams by real-time data reduction procedures. This structure of five equal size tracks is defined by the special requirements for the use of the CSM in connection with the Multi-Aperture Amplitude Interferometer.

\* skeletons

## 2. Individual Track Storage

Each of the separate tracks has a total capacity of 12,228 words. This is the maximum capacity of each track. In actual operation, one usually requires a predefined size for this memory which may be less than maximum. Thus the actual capacity in use for each track is selected by a thumb-wheel switch on the panel of the Circulating Semiconductor Memory. The capacity per track can be changed in increments of 1,024 words from 1,024 up to the full capacity of 12,228.

## 3. Individual Word Length

Each word in the memory has a length of 16 bits. When the CSM is operated in the disc mode, then the full 16 bits may be used for data storage. However, when the CSM is used in the CCD mode in which the CSM provides the information for scanning the Charge Coupled Device, then the least significant bit is used to identify that particular word as a control word or a data word. More detail of these functions is described in Appendix I. However, this means that when the CSM is used as the control for the CCD system, the actual storage is only 15 bits.

## 4. Operational Memory Rate

The Circulating Semiconductor memory will operate at data rates up to 5 megawords/second. Thus we have new words at the rate of 5 mega-words per second per track, or a total of 25 megawords per second. The rate of operating the Circulating Semiconductor memory may be adjusted using a thumb-wheel switch on the front panel. This selection provides the ability to operate at

5 MHz, 4 MHz, 2 MHz, 1 MHz, 0.5 MHz, .4 MHz, .2 MHz, .1 MHz and external. In addition, the rate is selectable from the minicomputer system through the interface. This capability permits the computer control program to slow down the operating rate of the memory to a speed at which it may perform a direct memory access transfer of data from the Circulating Semiconductor Memory to the minicomputer system core. Following this transfer, the minicomputer control program accelerates the memory to the data recording speed.

The external rate option permits one to drive the entire system at a rate which is characteristic of the target. This has some special applications in observing time dependent phenomena in a regularly rotating or pulsating source.

#### 5. Total Memory Capacity

Thus the total capacity of the memory consists of 5 tracks, each containing 12,228 words which have a length of 16 bits. Thus the total memory capacity is 0.978 megabits of memory.

#### B. Input - Output Structure

The input/output structure of the CSM consists of two different types of interface or "ports". The first is the camera input, which only receives data, and the second is the computer port which may either transmit or receive data.

### 1. Camera Port

The data is received from the Video Data Processor in five parallel streams of three bits. Each of these data words is to be added to the existing data in one of the tracks. Thus the total bit rate which is received by the CSM consists of three bits per track with each track operating at a rate of up to 5 MHz. Thus we are handling 15 megabits per second per track or an input data rate of 65 megabits per second.

### 2. Computer Port

The computer port transfers data from the CSM to the core of the NOVA minicomputer system. This operates under the direct memory access mode of operation of the minicomputer. The data may either be transferred from the minicomputer memory to the CSM, or from the CSM to the minicomputer. When the skeleton is being loaded, the system is operated under "disk mode" rather than the "CCD mode" which is the operating configuration during the CCD scan. These modes are switch selectable from the front panel of the CSM or the switch may be put into the software mode in which the mode is selected from the program in the NOVA minicomputer. The logic for selection of blocks within each track and the selection of which track to transfer is implemented in the circulating semiconductor. The direct memory access transfer is performed on 16 bit words at a rate of 0.5 megawords per second. Thus the data transfer rate between the minicomputer system and the Circulating Semiconductor Memory is 8 megabits per second.

### C. Logical Functions

The data which arrives from the video data processor proceeds to the "Arithmetic Logic Unit" (ALU). This permits one, under software selection, to either add the new information to the existing word, or to simply transfer



that information. The actual ALU's may be software controlled to provide 32 logical functions. However, these other logical functions are not implemented in this Circulating Semiconductor Memory.

#### D. Monitor Displays

Special display procedures permit one to observe the contents of the Circulating Semiconductor Memory. Digital to analog converters read the information in the control words and create rasters to drive an X-Y monitor oscilloscope. A third digital-to-analog converter transforms the data from the digital form to analog for Z modulation of the monitor scope. Thus one can get a two-dimensional display of the image which is contained in the memory. These are two selectable monitor outputs which may be directed from the front panel to any of the 5 tracks, thus 2 tracks may be monitored at the same time. In addition, there is a hardware computation of the fringe visibility, a quantity which is the practical, real time output of the system when used for the Multi-Aperture Amplitude Interferometer. The result of this computation is converted from digital to analog form and available for display on the monitor. Thus the latter will give the fringe visibility as it is being measured.

#### E. System Structure

The overall system of the CSM may be depicted by Figure 1.

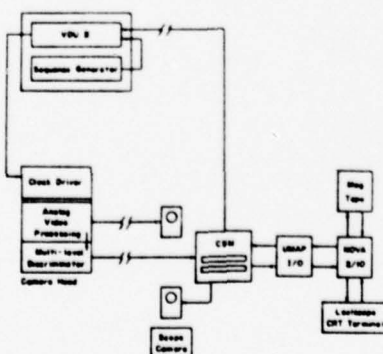


Figure 1

UMAP System Used in the Direct Imaging Camera Mode

Depending on the particular requirements of the observations, the scan rate, the format and the size of the array to be scanned is chosen by the operator. The parameters which describe this subarray are typed into the lexiscop CRT interface. The NOVA minicomputer then generates the detailed instructions which are required for scanning the CCD in this particular fashion. These commands are transferred and stored as special control words in the Circulating Semiconductor Memory. The CSM, which operates at a data rate as high as five megahertz, transmits these individual commands to the Video Drive Unit (VDU) which is located on the telescope near the photometer unit. The Video Driver Unit generates coded pulses to drive the CCD. The video output from the CCD, which contains the data, is brought to an electrically isolated portion of the camera head, i.e., separate from the chamber which contains the CCD drive circuitry. This configuration reduces the pick-up of coherent noise by the sensitive video electronics. The video signal is amplified and an A/D conversion is performed. The information in digital form is transmitted from the telescope down to the Video Processing Unit. The Video Processing Unit has a very simple function for the Direct Imaging Camera. However, in the MAAI, it performs the on-line computations which are required to transfer the data into a structure in which one may add successive frames of data. From the Video Processing Unit, the data stream proceeds to the Circulating Semiconductor Memory, where this data is added, pixel by pixel, to the data of the previous scans. For permanent storage of the data, the NOVA minicomputer slows down the CSM in a predetermined sequence, transfers a block of data from the CSM to the NOVA core storage, sets the registers in this block in the CSM to zero, and accelerates the CSM to the proper rate and reinitializes the CCD. The data is then transferred from the NOVA core storage to digital magnetic tape while new data

from the CCD is being recorded in the CSM. (The special I/O card and a special data translator interfacing the NOVA are described in the University of Maryland Technical Report # 76-098).

#### F. Current Status

The memory is in 4K boards. At present, there are 12 such boards so one may either operate 4 tracks full or 5 tracks with 8K. In this mode it has been operating for about two years quite successfully. After the initial break in, the major problems have been chip burn out; after the initial installation of the CCD's and the initial operation, there have been several shift register chips which have become non-operational. These are located with some difficulty since the data passes through all chips on the board. However procedures have been developed to evaluate and locate the faulty shift register.

The few upgrades of this instrument would be worth while but have not been performed at present. These consist of:

1. Rewiring of thumbwheels to provide a more operator-oriented coding
2. Provide extra boards for spares and to permit image processing (two additional boards have been provided by another agency)
3. Provide clock outputs to drive other systems
4. Provide an input for clock signals

These modifications, although desirable, have not been considered sufficient to interrupt the use of the system. The major effort at present

has been the further programming for special applications.

Most of the operation has been at 1 or .5 MHz. Tests have been conducted at 2 and 4 MHz where it appeared operating successfully. 5 MHz may draw sufficient power to be a somewhat borderline operation. This unit has been transported and by air freight and survived.

#### G. Next Generation

A number of suggestions have arisen for a next generation instrument. However, many of these are incorporated into the CCDCSM which has now been fabricated. Thus a report on this will be coming out soon in which the next generation improvements are discussed and their implementation feasibility considered.

Basic parameters of this new generation system consist of:

1. Single track
2. 8 MHz operation
3. 24 bit words
4. 64 K words expandible to 256
5. By CCD change expandible to 1 megaword or 24 megabits
6. Low power consumption
7. 16 selectible logical functions for input data



### III. SINGLE SCAN DATA RECORDING SYSTEM

A considerable amount of the data for these tests was recorded with a single scan data recording system. This consists of a computer/University of Maryland Array Photometer combination which can convert the analog video signal at each pixel into an eight-bit digital word at a 1/2 MHz scan rate. We will also operate at a rate of 4 MHz with some modification. However a large amount of this data has been gathered at 0.5 MHz. The single scan data recording system will typically record every 10th frame and write it to magnetic tape. This is particularly useful for detailed analysis of the data, as for example, the evaluation of pulse height distributions and the gain of the system. The single scan data recording system has been written up in more detail in a University of Maryland document.

#### IV. FRAME ADDITION

This task addresses the summation of many frames in order to examine subtle effects not visible on a single frame. This would be performed in software using the recorded frames. This has been achieved with programs which were transferred from an image processing system developed by the Amplitude Interferometer Program to a set of programs which will handle in an interactive fashion the data from the CCD. These programs are configured in a way that will permit the minicomputer to run many hours unattended in performing the averaging and other operations.

As discussed earlier, a portion of this work has been dominated by the lack of the fully operational ICCD. This work has been performed by an ICCD borrowed from Goddard Space Flight Center but which does not have the low leakage current which we need. Using this we have recorded data on magnetic tape on each frame. This has been done both with the CCD and the ICCD.

The tests with the CCD demonstrate a systematic noise and a correctability at the 100 electron level.

We have, for example, used the ICCD on the 36-inch telescope at the Goddard Optical Research Facility (GORF) and the 200 inch at Palomar Mountain. For example, Figure 2 is an image of a globular cluster (M3) recorded on the 200 inch telescope at Palomar Mountain. This figure illustrates a typical array (or analog) frame with the dark subtracted. This is formed by successive summing, so these figures are the average of 100 repeatedly scanned frames.

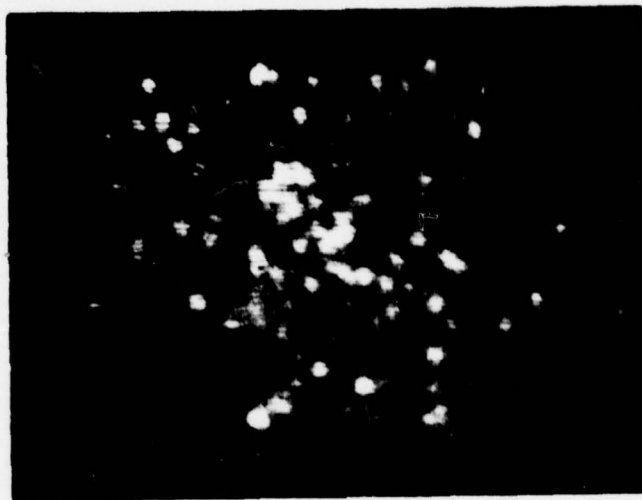


Figure 2

Linear Digital Display of M3

By this procedure we have now reduced the effect of the read noise by a factor of 10. In order to see the dynamic range of this data more clearly, Figure 3 is a logarithmic display (generated in the UMIPS). Thus we see here the capability of recording this detailed data for study.



Figure 3

Logarithmic Digital Display of M3

# V. SINGLE PHOTOELECTRON DETECTION

We may now use this same data recorded in a single scan data recording system for single photoelectron discrimination. Let us first use a special program within IPS to obtain the pulse height distribution. For the case of M25, we have the following distribution

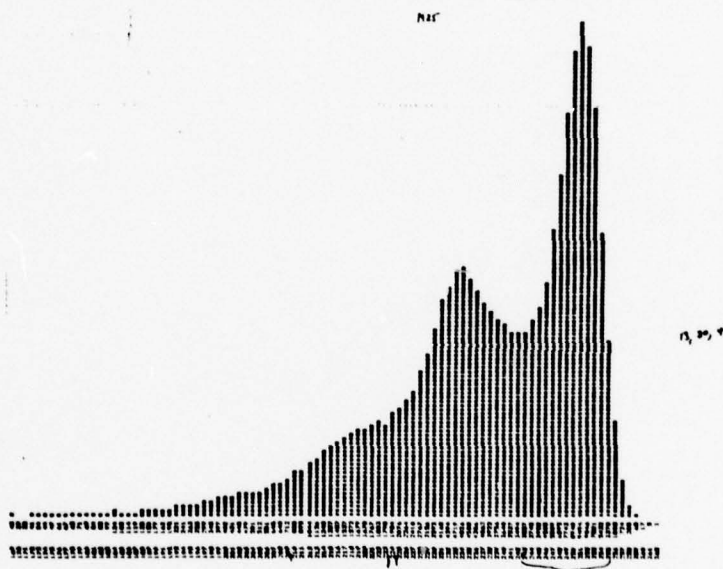


Figure 4

Pulse Height Distribution for CCD Image of M25

Thus we see we can set a discriminator at an appropriate level and rather clearly distinguish between no/one photoelectron. Doing the discrimination in the computer on the data from M3, we obtain the following image



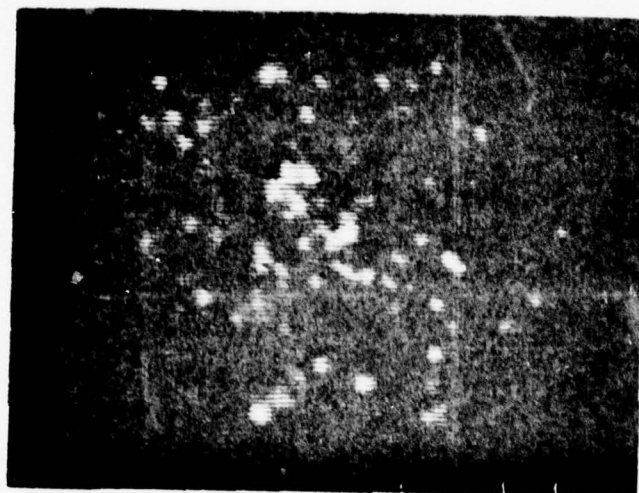


Figure 5

Discriminated Digital Display of M3

## VI. SKELETON AND SCANNING PROCEDURE

In this section we generally describe the capability of scanning and selecting format and repetition rate. In order to provide a reasonable description of the overall system, the technical discussion will address certain aspects of the system many of which were supported under this contract. However, other portions were supported elsewhere.

### A. Basic Procedure

As was discussed in the previous section, the Circulating Semiconductor Memory has the capability of recognizing words in which the least significant bit has a value 1 as control words. It is the decoding of what is contained in the control word which causes the CCD to scan. Thus, there are, in effect, commands to start scanning a new line and to transfer the image in one field from the photo-integration sites to the transfer registers, instructions to transfer this image out etc.

### B. Control Word Structure

The control words provide the instruction for scanning. The function of the bits within these words is detailed in Appendix I.

### C. Subscanning Option

For various applications we wish to scan the portion of the array. Thus operating at a 1 MHz rate for example one may subscan into a shorter integration time. This may be used for a variety of purposes

1. Higher time resolution
2. Larger dynamic range.

We shall discuss both of these advantages; however, in this section we shall concentrate on the latter.

Since we have control of the transfer of the image from photo sites where the integration occurs to an external location, we have the ability to subscan the smaller array. This will overlay all such units on the array. Thus if we subscan in four quadrants the ultra-array will be the superposition of four quadrants. Thus for most applications one has to control the light so only one quarter of the array is illuminated. However, this is often the case for our configuration where we are observing the single satellite or stellar object and the rest of the field is dark or has only sky background, or much fainter stars.

#### 1. Objectives

Objectives of the subscanning is to provide better control of saturation for direct imaging and higher scan rates for both temporal phenomena and to increase dynamic range.

Some of the advantages of subscanning are:

1. Higher frame rate
2. Greater dynamic range
3. Pulsar effects
4. Lower memory requirements
5. Faster transfer to permanent data storage.

The disadvantages are primarily the need to do optical aperture.

#### 2. Implementation

In order to implement the partial scanning, we require a program to load the information into the circulating memory and we need a program for the actual running of the integration. In order to load the proper scan program or skeleton into the CSM, a special program must be created in the minicomputer which addresses the Circulating Semiconductor Memory. This program has an input the length of each line, the number of lines, the number of units at the end of each

line. Its output is an sequence of individual commands. This program has been implemented on the NOVA 2-10 which is interfaced to the CSM. An example of a skeleton generating sequence by this program appears as Appendix II. These have been implemented on the NOVA. The creation of a new skeleton is a manual operation which will typically require half a day for generation. At present we have skeletons at the following points:

a. Full frame

This is a one hundred twelve pixel by one hundred and one line skeleton which is used to display the interlaced two fields of the 100 x 100 array the CCD 201 and 202.

b. 8 K field

This is an array which scans out two-thirds of the array. This is the actual skeleton required for the MAAI very large telescope. It is the upper limit of the MAAI operation. It has also been used to make absolute measurements of leakage current in ICCD's.

c. One quarter array

This subscanning skeleton provides one quarter of the array. It has been properly debugged and a display procedure created which utilizes the frame.

d. Ten by ten

The ten by ten array provides very high increase in dynamic range. It also produces very rapid scanning for high frequency phenomena. The normal scan rate for this is 3,000 frames per second with the option of going to 32,000 frames per second.



#### D. Time Resolution

In a related development, the time resolving ability of this system is demonstrated. The time resolution was developed separately. In this mode we record several phases, for example the six phases found in the ten by ten skeleton. The flashing of a pulsar may be at a rate above the ability to scan using a full frame scan. However running the ten by ten skeleton may allow scanning the chip fast enough to run the six phases of the scan in synchronism with the pulsar. Each phase will coherently add the light at that phase of the pulsar's cycle; thus we have increased the time resolution.

## VII. DEMONSTRATION OF PARTIAL SCANNING PERFORMANCE

We shall now discuss the data arrays which have been developed in order to demonstrate the performance of the partial scanning procedures. In order to demonstrate the procedure of partial frame scanning, several examples will be discussed. We use the entire frame scan, the quarter frame scan and the ten by ten scan which have been discussed in an earlier section.

### A. Data Recording Modes

For using the data, there are two modes of data recording. The first of these consists of the use of the Single Scan Data Recording System in which each pixel is digitized and the value of each pixel is separately recorded. The second procedure is the integration mode in which a part of the scan is accumulated in the NOVA minicomputer core and then the total picture transferred to magnetic tape.

The third mode is direct observation of the video from the camera head with no integration. This is the "video monitor" mode.

### B. Unresolved Images

We consider a series of tests which uses an input to the CCD which is equivalent to an unresolved light source. In actual fact, it was chosen to extend over several pixels, but is basically a point source reasonably sampled.

#### 1. Full Frame, 44 Hz

In Figure 6, we see a representation as viewed on the "video monitor" of the result of observing with no light input. Thus we see a dark frame which should be uniformly dark. However, there are some background fluctuations which, as we shall see, subtract out with high precision. In addition, there are effects which cause the columns on the extreme left and right to be bright.

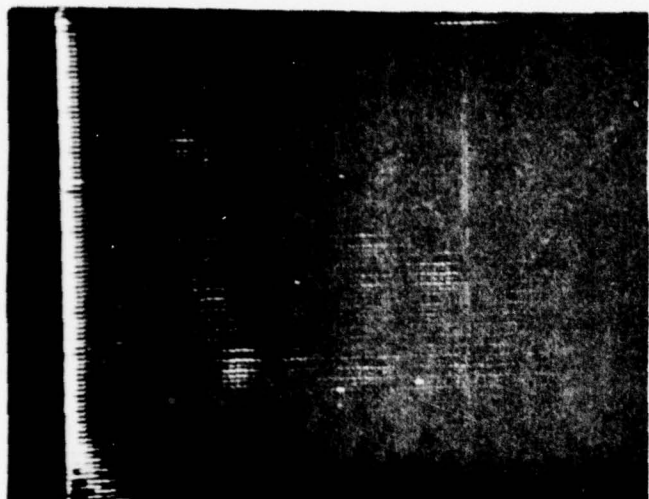


Figure 6

Monitor Display of Dark Current

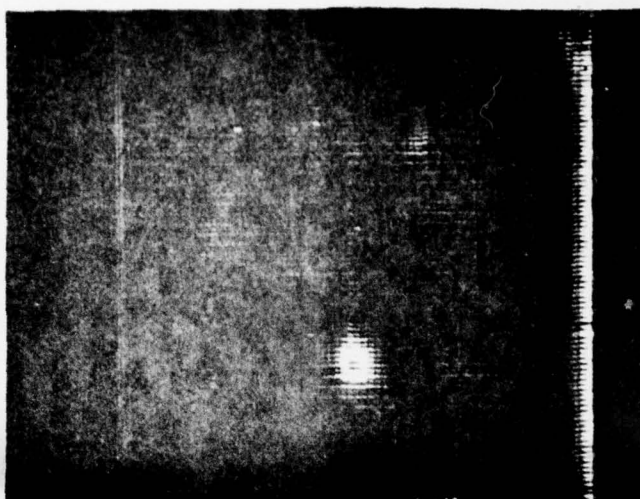


Figure 7

Monitor Display of Overexposed Point Source

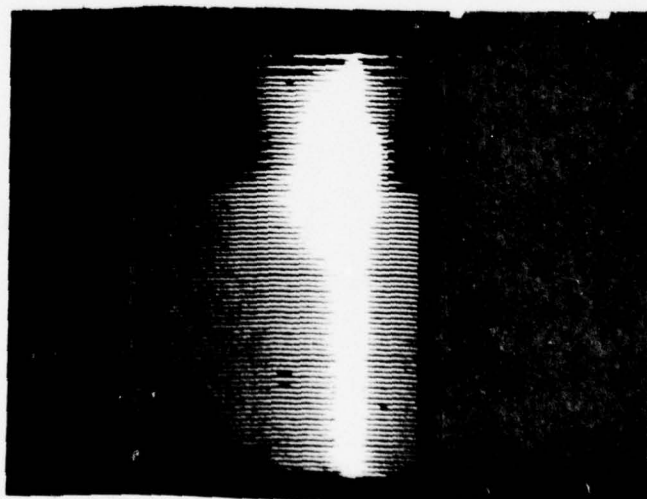


Figure 8

Digital Display of Overexposed Point Source

We now observe Figure 7 with an unresolved point object. As we can see at this level of brightness there is strong blooming. This shows in two separate modes, as discussed in the paper of Appendix III. One of these is a form of radial blooming which extends the basic object. The other is vertical blooming which is responsible for the line which goes from the top to the bottom of the screen.

Each of these are obtained from the monitor scope and therefore represent no integration and no subtraction.

At the same time that each of these arrays was observed on the monitor, they were also recorded using the single scan data recording system. In each case, 100 frames were recorded. Withing the computer, these 100 frames were averaged. Then the averaged dark frame was subtracted from the averaged illuminated frame.

In order to display this to show an optimal amount of information for photon limited pictures, we used a "square root display". In this case, we take the square root of the image and then with proper multiplying factor, we find that the noise occupies the same part of one grey level whether the image is at full brightness or dark. This is true for photon noise.

The square root display on our monitor of the subtracted image is shown in Figure 8. This is an expanded version showing the problems in Figure 7. On either side of the image, we see another effect, a negative blooming, which is the result of saturation in an amplifier. Most of this has been removed. One thing to note is that the dynamic range in this picture is over 1,000 between the dark areas on either side of the image and the image itself.



In evaluating the magnitude of these phenomena, it is well to note that the difference in intensity between the brightness of the spot and the brightness of the least detectable change in the frame is about  $6 \times 10^6$  in this display.

2. Quarter Frame, 330 Hz

We now load a separate skeleton into the CSM and scan the CCD using four superimposed separate arrays with the same light source brightness. The scan rate is now 330 frames per second. Even with this increase in the scan rate we are still unable to escape the blooming although it is less severe.

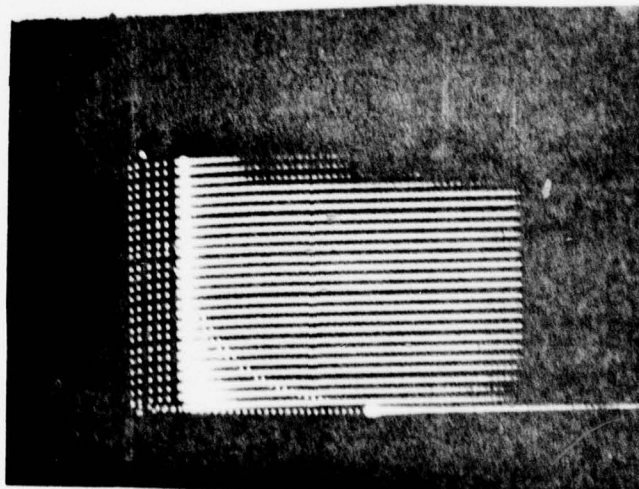


Figure 9

Quarter Chip Scan Dark Current

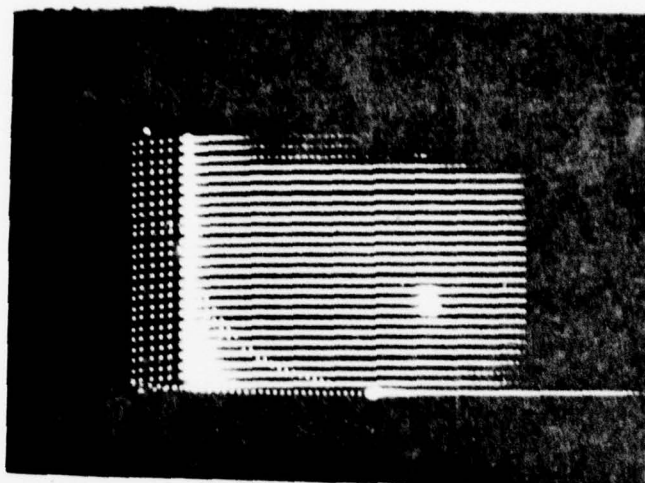


Figure 10

Quarter Chip Scan of Overexposed Point Source

Again we have the monitor displays for the image and the dark. The subtracted result consists of Figure 11.

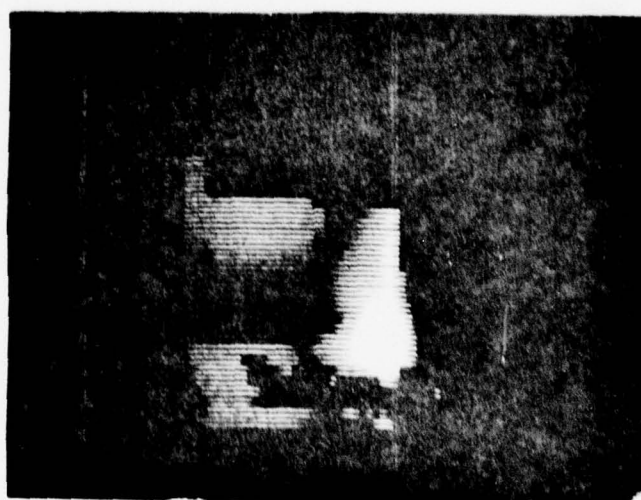


Figure 11

Dark Subtracted Point Under Quarter Scan

where we are again dominated by saturation phenomena. The bar to the left consists of an overshoot due to the strong saturation. The large part of this has been corrected in later cameras. However the basic blooming is the result of over filling the wells and cannot be bypassed, in this CCD structure.

Some of the structure seen in this array which has a range of about  $1.5 \times 10^6$  is due to the folding. Thus on the extremely dark regions, we have folded the edge problem into the center of the array. Problems which occurred on the previous image and on the edge are not intruding farther into the apparent image due to the reduction by a factor of 4 in dark current. However, we again should note that the least significant level change on here is extremely small.

### 3. Ten by Ten Array, 3 KHz

In this section we discuss the results which have been obtained with the ten by ten array. In this mode we are operating at 3,000 frames per second. However, let us first observe the point source directly on the monitor.

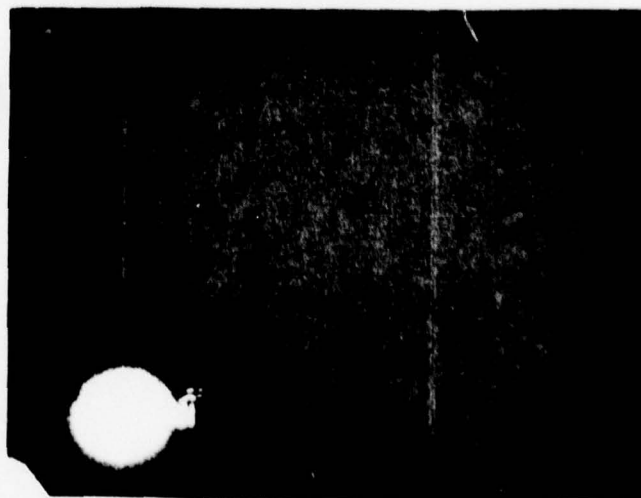


Figure 12

Tenth Chip Scan of Overexposed Point Source

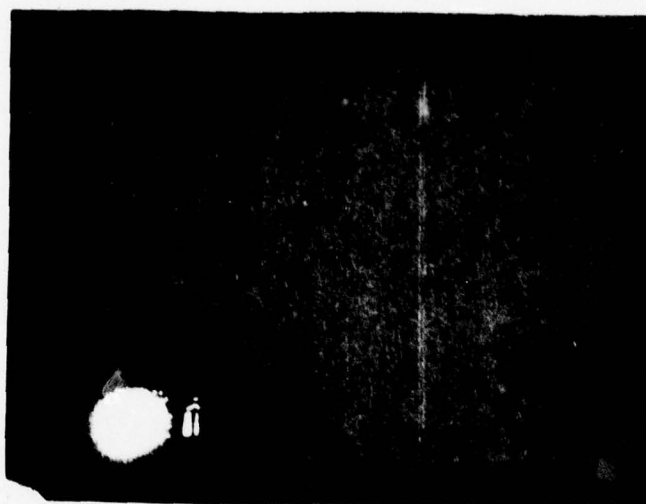


Figure 13

Tenth Chip Scan Dark Current

We note here the effect of over exposure in the monitor. This is not saturation of the CCD or the data electronics, but it is saturation of the phosphor on the monitorscope. This could have been readjusted but in this particular set of sequences, all brightness levels of sources and all settings of displays were left unmodified to provide a comparison that is uniform throughout.



Here Figure 12 shows the effects of the light source on the array and Figure 13 is the array without the light source i.e., the dark pattern. This data was taken directly from the monitor scope so it consists of a single scan. It is thus much more noisy than we might expect with later display and it suffers from the monitor display problems.

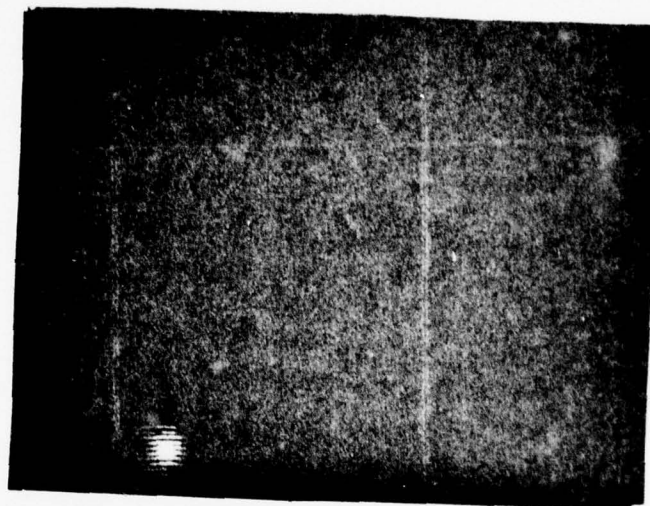


Figure 14  
Digital Tenth Chip Scan of Overexposed  
Point Source

In Figure 14 we see the digital subtraction of image 12 and image 13. Once again we see the very strong saturation phenomena of the CCD. Note that the CCD has a dynamic range of about 3,000 prior to saturation. We have used a special display in the amplitude interferometry image processing system which permits one to observe the photon noise at all levels. Thus this picture is a "square root" picture in which the intensity of each point is taken by the square root. Thus the noise level at any image brightness has the same number of grey scale levels. This gives us high sensitivity for faint parts of the image without resulting in excess noise contributions.

#### C. Partial Frame Scan Using Satellite Images

The target under discussion above has been an unresolved element. We now address the question as to whether the same kind of results may be obtained with an extended object. For this, we use an image of the DSCS II satellite. These images, and their brightnesses, are roughly comparable to what one would see at the AMOS 60-inch telescope with a reimaging optics to match the CCD properly to the compensated imaging system and if the satellite were in a low orbit at about 10 megameters.

Thus we see in Figure 15 an image of the DSCS II as it would appear on the monitor, and in Figure 16 we see an image as it appears after processing with the square root display. One will readily note that the image quality is not high. This is primarily the result of our data processing procedures being developed to work with digital data and taking advantage of the full accuracy of the data rather than a display mode. Thus the quality

of this picture is not as bad as it seems given that a magazine drawing of the satellite was photographed to produce a transparency which was projected onto the CCD. The CCD image was then displayed on a non-linear phosphor on the monitor which was photographed with poloroid film and then xeroxed for this.



Figure 15

DSCS II Monitor Display

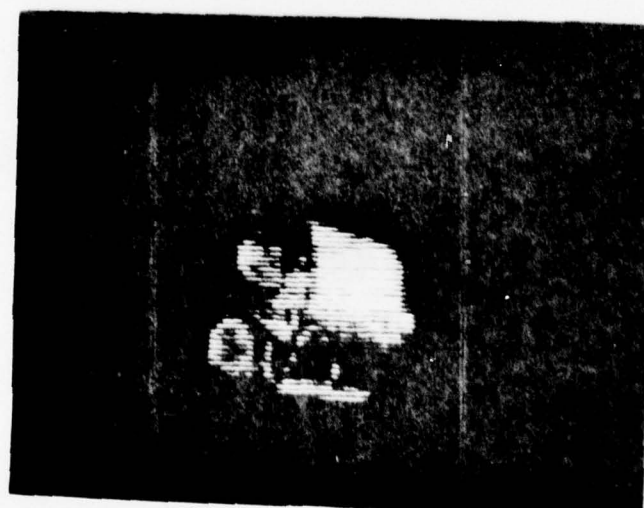


Figure 16

DSCS II Under Digital "Square Root" Display

However, this is equivalent to viewing the satellite through a neutral density filter to reduce its brightness. If we display the image in its full brightness, then we obtain an image of the form shown in Figure 17. Once again, we see in Figure 18 the digitally subtracted image with enhancement of the low signal levels.

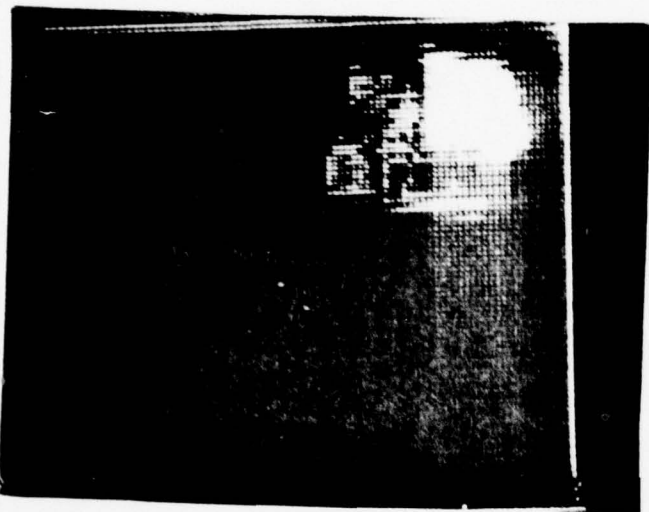


Figure 17

Monitor Image of Bright DSCS II

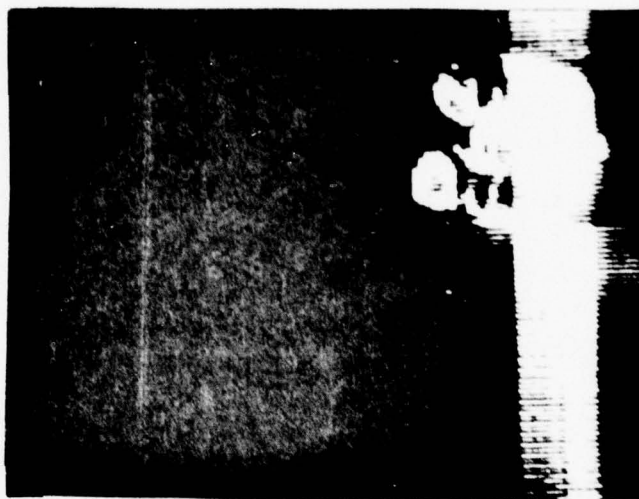


Figure 18

Digital Display of Bright DSCS II

#### 1. Quarter Frame Scan

We now load in the new scanning skeleton and with the same brightness of the satellite, which is its expected brightness with a compensated imaging sensor, we see that the images do not show the vertical blooming seen with the full frame scan. Once again the adjustments for optical passage through the phosphor/poloroid/xerox have not been chosen particularly well but it does clearly indicate the disappearance of the blooming.

For the full frame we have



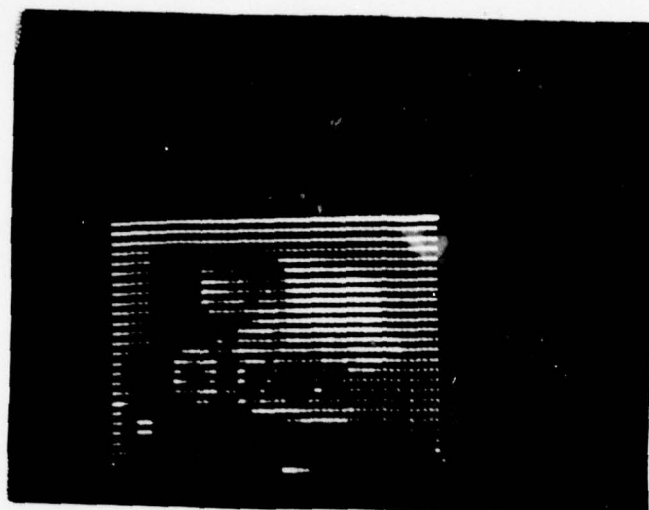


Figure 19

Quarter Chip Scan of Bright DSCS II

and for the subtracted result we have



Figure 20

Digital Quarter Chip Scan of Bright DSCS II

We now have looked at the monitor display of the one quarter scan. Here we have an image of a satellite which once again has been adjusted into a blooming region. The scan image is now operated at 4 times the rate and the blooming has vanished. The light intensity has not changed between these two images. Note that all of these exposures have been from the monitor and they are therefore analog pictures. However, the same phenomena will apply to the photon counting pictures and will increase the dynamic range in the same manner. We may now identify the brightness of the different levels, even on the non-linear display of the oscilloscope.

## PROGRAM CONCLUSIONS

### A. Array Measurements

The performance of the Single Scan Data Recording System is demonstrated in the images discussed earlier. These were recorded in the laboratory and on various telescopes.

The Single Scan Data Recording System has been developed to provide the ability to record data at 4 MHz.

The IO display has been developed in a slightly different fashion than originally proposed but the photographs displayed here were all taken on a monitor either on the video stream or in a mode in which the picture was transferred to the CSM and then developed. A separate display for the information NOVA case (integration mode) has also been developed.

### B. Hardware Developments

The existing memory boards have been modified to provide the capability discussed in the proposal. Additional integrated circuit boards have been fabricated which yield the full 8196 words per track. This is operational and has been demonstrated. Some of these boards were in use for the pictures shown in the technical sections, we have, for example, Figures 16, 18, and 20.

The CSM has been operated for the display of data used in sensor evaluation. Thus most of the poloroids displayed in this report were taken from the CSM. The CSM also has provided the drive for the CCD, for the partial scanner.

Thus these mean two objectives have been satisfied.

C. Evaluate the Successive Frame Addition

The post processing addition of frames from magnetic tape was performed.

The generalized NOVA program to create skeletons in the CSM was created and this has been used to permit frame addition (at the three bit level) and partial frame scanning.

In order to do the photon counting, integration with the three bit data an ICCD with low leakage current is required. Such a device has not yet become available so this portion has not yet been completed.

D. Controlled Frame Size

For this goal, we have used the frequency dependent CCD drive in the video circuits to change the size of the scan format. This was performed and discussed under the technical section. This test was performed and evaluated in the technical discussion.

E. Data Evaluation

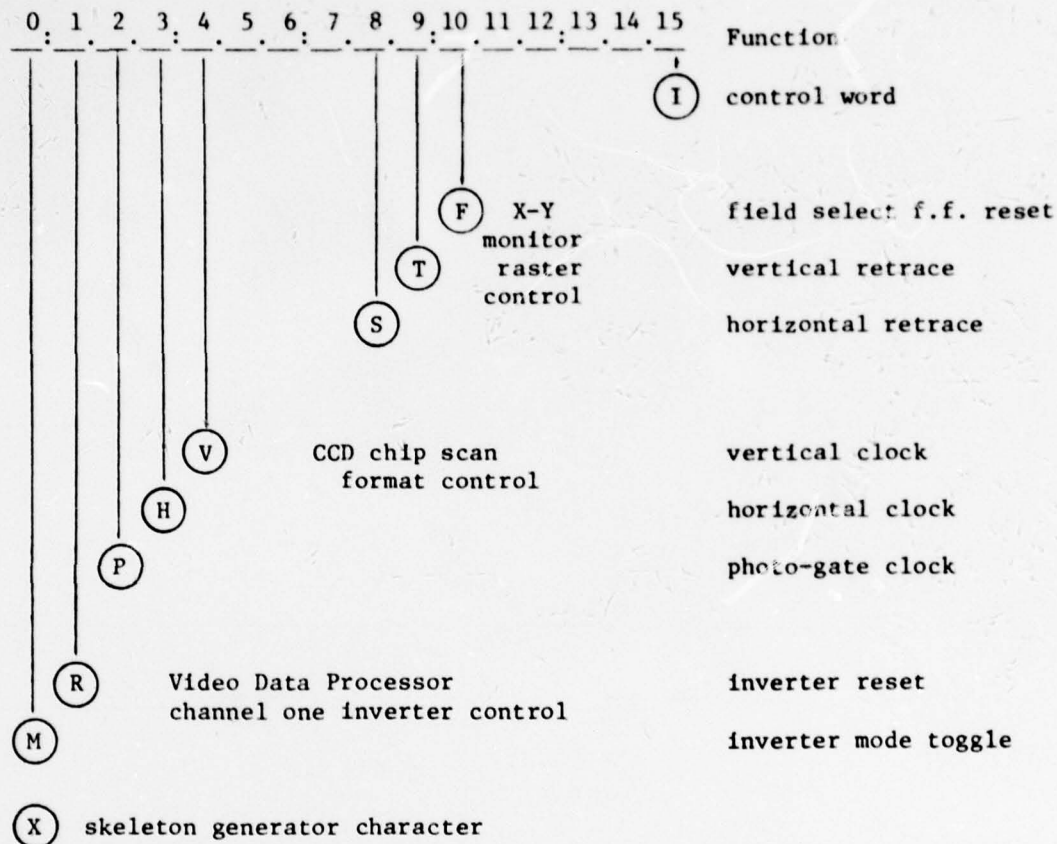
The data evaluation was done both on the Univac 1108 and on the University of Maryland Amplitude Interferometry Program Image Processing System. The latter is a dedicated system which permits the processing of this data in quasireal time.



## APPENDIX I

CSM CONTROL WORD FORMAT

## CIRCULATING SEMICONDUCTOR MEMORY CONTROL WORK FORMAT

Sample skeleton generator function

Input text: 2[1,2,F,ST,3(0)],77

Output octal data: 1,2,40,300,0,0,0,1,2,40,300,0,0,0,77

## APPENDIX II

## SAMPLE SKELETON SEQUENCES

PRIMARY SKELETON FOR FULL CCD SYSTEM  
100 ROW BY 100 COLUMN CCD ARRAY  
INTERLIEVED TWO FIELD TV RASTER  
FULL LINE INVERSION ON CHANNEL ONE  
REQUIRES 11K OF CSM MEMORY  
(WITH 32. WORDS DEFAULT FILLED) '

4(IHV),99(FPVHTSI),5(PVHI),  
IHPVR,2(IHPV),I,100(I),IS,3(IHV),  
50CIHM V,2(IH V),I,100(D),IS,3(IHV)],  
4(IHV),99(PHTSI),5(PHI),  
IHRPM,2(IH V),I,100(I),IS,3(IHV),  
50CIHM V,2(IH V),I,100(D),IS,3(IHV)]'



SKELETON FOR HALF CHIP CCD SYSTEM  
 50 ROW BY 100 COLUMN CCD ARRAY  
 INTERLIEVED TWO FIELD TV RASTER  
 FULL LINE INVERSION ON CHANNEL ONE  
 REQUIRES 6K OF CSM MEMORY  
 (WITH 312. WORDS DEFAULT FILLED) '

```
4(IHV),99(FPVHTSI),5(PVHI),
  IHPVR,2(IHPV),I,100(I),IS,3(IHV),
25[ IHM V,2(IH V),I,100(D),IS,3(IHV)],
4(IHV),99(PHTSI),5(PHI),
  IHRPM,2(IH V),I,100(I),IS,3(IHV),
25[ IHM V,2(IH V),I,100(D),IS,3(IHV)]'
```

```
;NOTE: THIS ASSUMES GOOD RESULTS
;       FROM THE MIX DUMPING MODES
;       AS IT USES THE SHIFT REGISTERS
;       TO STORE THE LOWER HALF FRAME

;       THIS SKELETON MIXES PHASES
;       OF (VERTICAL) CHIP HALVES
```

TRY AND SCAN ONE TENTH THE CHIP

1 K CSM MEMORY--NO INVERSION

\*\*\* NO CSM DIRECTORY MAP \*\*\*

good only for single scan system use

LINEC: 13. FIELD: 1 TOP TRASH 0

FELD1: 2 LINE: 1 BOTTEM 0

FELD2: 84. GROUP: 12. LEFT 2

FELD3: 86. COUNT: 1 RIGHT 3

6[13(IHPVT),IH,5(IHVS,13(I)),

13(IHPTF),IH,5(IHVS,13(I)),2(IHPV)],4(IHPV)'

;6 PHASES TO THE CSM

; PROPER SINCE IT IS 50 LINES HIGH--

; 5\*10.

## APPENDIX III

ON A PHOTON COUNTING ARRAY USING THE FAIRCHILD CCD201

ON A PHOTON COUNTING ARRAY USING  
THE FAIRCHILD CCD201

Douglas G. Currie

Technical Report 75-082

May 1975

UNIVERSITY OF MARYLAND  
DEPARTMENT OF PHYSICS AND ASTRONOMY  
COLLEGE PARK, MARYLAND



## ABSTRACT

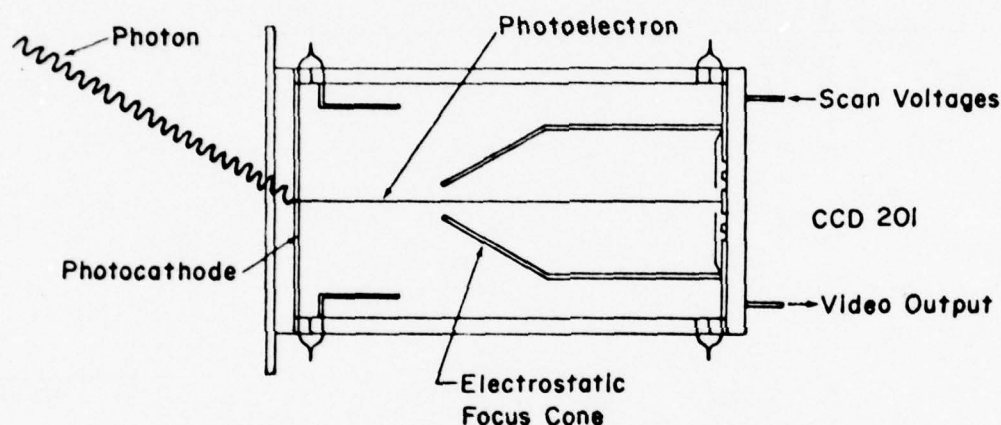
An internally Intensified Charge Coupled Device (ICCD), using a semi-transparent photocathode and front illuminated Fairchild CCD201 is described. A light detection system incorporating the ICCD should ultimately permit single photoelectron discrimination at a scan rate of about 350 frames a second. This will provide a data rate which is an order of magnitude larger than comparable systems. Such a device, the first of this type, has been fabricated by the Electronic Vision Company and recently tested at the University of Maryland. The tested unit, after being sealed off, had a good photocathode and the CCD operated properly after the bakeout procedure. Successful measurements of video noise, electron gain, penetration of the transfer registers, and damage to the CCD were conducted. Before becoming gassy, this tube performed acceptably in the critical areas as an intensified television camera for the low light level detection. Although single photoelectron discrimination was not possible due to excess random noise, the results of the tests indicate that the expected single photoelectron operation is feasible. Another ICCD has been fabricated which has solved some of the problems found in the first device.

## TABLE OF CONTENTS

I. INTRODUCTION . . . . .	1
II. PHOTO-SENSOR REQUIREMENTS. . . . .	3
Amplitude Interferometer Requirements . . . . .	3
Imaging Camera Requirements. . . . .	3
III. METHOD OF CCD OPERATION . . . . .	4
Theory of Operation of the CCD . . . . .	4
Operation of the CCD . . . . .	4
Noise Sources in the Charged Coupled Device . . . . .	4
Random Charge Noise . . . . .	5
Thermal Leakage Current . . . . .	5
Thermal Leakage Noise. . . . .	5
Array Display . . . . .	6
IV. OPERATION OF INTENSIFIED CCD . . . . .	7
Theory of Intensification . . . . .	7
V. ADVANTAGES OF SINGLE PHOTOELECTRON DISCRIMINATION . . . . .	9
VI. SATURATION, BLOOMING AND LAG . . . . .	12
Saturation . . . . .	12
Blooming. . . . .	12
Radial Bloom. . . . .	12
Vertical Bloom . . . . .	13
Horizontal Bloom . . . . .	13
Lag. . . . .	13
VII. DAMAGE MECHANISMS. . . . .	14
VIII. TEST SYSTEM DESCRIPTION . . . . .	15
IX. OPERATING DATA SYSTEM . . . . .	18
REFERENCES . . . . .	20

## I. Introduction

In the following we discuss the work being done at the University of Maryland on the internally Intensified Charged Coupled Device (ICCD). The details of the actual tube, which is being fabricated by the Electronic Vision Company will be described in detail in a later talk by John Choisser. The ICCD will be operated as a photon counting array detector. The basic configuration of this tube is indicated in Figure 1.



Schematic Diagram of Intensified Charge Coupled Device

Figure 1

An incident photon is converted to a photoelectron with a standard photo-cathode (S-20, for example). This photoelectron is then accelerated to an energy of about 15 Kev and electrostatically focused onto the front surface of a Fairchild CCD-201. Within a particular photosite on the CCD the photoelectron creates many hole-electron pairs by ionization. These charges from the single photoelectron are collected and produce an easily detectable charge packet. These charge packets are "scanned" from the CCD by the conventional clock pulse trains.

After on-chip amplification, the signals leave on a single video output line. This data is then electronically processed to detect the charge packet produced by each photo-electron. The information is then processed on-line, and stored in a special memory which can operate at video data rates.



## II. Photo Sensor Requirements

This development effort with the ICCD is motivated by two different applications with significantly different requirements.

### A. Amplitude Interferometer Requirements

The primary application of the ICCD will be as the light sensor for a particular instrument, the Multi-Aperture Amplitude Interferometer (MAAI). This instrument is a multi-channel version of a similar instrument which has been used in an astronomical observation program over the last few years<sup>1,2,3</sup>. Basically, this application requires an array of photosensors, each of which acts as a photo-multiplier. The requirements are:

1. The ability to discriminate on single photoelectrons
2. The scan of an entire frame in a few milliseconds
3. Very low lag, or memory from one frame to the next frame
4. Minimal cross talk between spacial channels (or pixels)
5. The ability to distinguish reliably among zero, one, two, or more photoelectrons per pixel per scan.

### B. Imaging Camera Requirements

The other application, which is related to the MAAI, consists of an imaging camera in the focal plane of the telescope or the spectroscope. For this application, the requirements consist of items 1, 2, 3, and 4 listed in section A, as well as:

1. Very large dynamic range
2. Very low blooming

The electronic operating conditions for the ICCD will be somewhat different in order to satisfy the different requirements of the two applications.

### III. Method of CCD Operation

#### A. Theory of Operation of the CCD

The Fairchild CCD-201 will be bombarded by electrons arriving in the front of the CCD. The transfer registers, which carry the charge from the photo-sensitive sites to the on-chip preamplifier, operate independently and at the same time as the integration of charge at the photosites. Thus the transfers or "scanning" can take place during the integration period, and the array is sensitive essentially all the time. These transfer registers are protected by a layer of aluminum, so that the bombarding electrons cannot produce any ionization or "noise" in the registers. In the operational data system, the scanning procedure is controlled by an external device (the Circulating Semi-conductor Memory (CSM)) which may be programmed to scan a portion of the 100 x 100 array, or the entire array.

#### B. Operation of the CCD

In order to operate the light sensor on the telescope, a long cable from the electronics to the camera head is required. To handle this, a special camera head has been fabricated which minimizes the cross-talk and coherent noise. The pulse trains are transmitted to the telescope on high impedance lines. These are converted to the required high current pulses by clock drivers in the camera head. The camera head also contains amplifiers, a sample and hold circuit and a discriminator.

#### C. Noise Sources in the Charged Coupled Device

There are three types of electronic noises which are most significant with respect to ideal photoelectron discrimination operation. These are "random charge noise", "thermal leakage charge" and the variation of the thermal leakage current or the "thermal leakage noise".

### 1. Random Charge Noise

The random noise is indicated by the variation of the voltage level, from one frame to the next, at a given pixel. For measurements of the random noise, the illumination is presumed to be constant, or as for most of these tests no illumination. The random noise is characterized by the standard deviation of the voltage at a given pixel for a number of successive frames. This type of noise behaves as if it were Johnson noise dominated by the capacitive input of the on-chip preamplifier. The value of the random noise is essentially independent of temperature (more precisely it varies inversely as the absolute temperature). At a data rate of 0.5 MHz the random noise has been measured by Dyck and Jack<sup>4</sup> to be about 300 electrons per pixel per scan.

### 2. Thermal Leakage Current

This "dark current" or thermal leakage current is due to thermally generated charge pairs which are created within the active silicon. The leakage current is parameterized by the average number of electrons which collect at a given pixel during the integration interval (usually the scan or frame time). The value of the thermal leakage charge varies across the frame from pixel to pixel. It decreases by a factor of two when the temperature of the CCD is reduced by 6 or 7°C and decreases linearly as the integration time is decreased. The average leakage charge across the frame does not significantly effect the ICCD operation but its variation across the chip may create a problem. The variation of the thermal leakage charge from frame to frame (Poisson noise) would properly be a component of the random noise, but its value is negligible for normal ICCD operation.

### 3. Thermal Leakage Noise

The thermal leakage noise is the variation of the thermal leakage charge across the array. This will be parameterized by the standard deviation of the thermal leakage charge across the array.

More precisely, it is the variation of the mean (over many frames) thermal leakage charge across the array. This latter form of the definition removes the random noise as a component of the thermal leakage noise. It should decrease with temperature at the same rate as the thermal leakage charge and decrease in proportion to the increased data rates. In order to permit single photoelectron discrimination without a change of discriminator level for each pixel, this noise must be reduced to about 100 photoelectrons. This may safely be accomplished by cooling to approximately  $-20^{\circ}\text{C}$ .

#### D. Array Display

In order to study these quantities an Image Processing System has been developed at the University of Maryland which permits computer processing of many scanned frames and the determination of these quantities by a standard procedure.



#### IV. Operation of Intensified CCD

##### A. Theory of Intensification

The photoelectrons provided are accelerated to 14.6 KeV prior to impact on the CCD. This value is sufficient to produce sufficient charge by ionization to permit the detection of a single photoelectron, but is not sufficient to penetrate the aluminum (and other layers) which form the protection for the transfer registers. Since different regions covering the transfer registers have different thicknesses, the accelerating voltage is chosen so the photoelectron cannot penetrate the thinnest region. In fact, the energy has been further reduced so the photoelectron will not penetrate into the final layer of  $\text{SiO}_2$  insulation above the active silicon of the transfer registers. For a photoelectron which impacts the CCD over a photosite, some of the energy is lost in the layers of silicon and silicon dioxide which lies over the photosite. The 14.6 KeV electron will encounter either of two regions over the photosites which have different thicknesses. Therefore, the photoelectron may have either 8.5 or 9.6 KeV upon entry to the active silicon. These detailed calculations are based on a specific model of the CCD architecture which was obtained from R. Dyck of the Fairchild Corporation. For any given device from a particular run, it is expected that there will be significant variations. Thus these numbers may be considered as a sample calculation.

As a result of the energy of the photoelectron entering the active silicon, we will have the production of charge packets containing 2300 or 2600 electrons, depending on how many layers it has penetrated. The variation of these numbers is relatively small, especially when compared to noise in the on-chip amplifier of 300 electrons. Since the incident electrons may enter either area, we expect an ideal pulse height distribution of the electrons to have the form indicated by the vertical bars in Figure 2. The cross hatched area represents the pulse height spectra for the case in which the noise of the on-chip preamplifier is included.

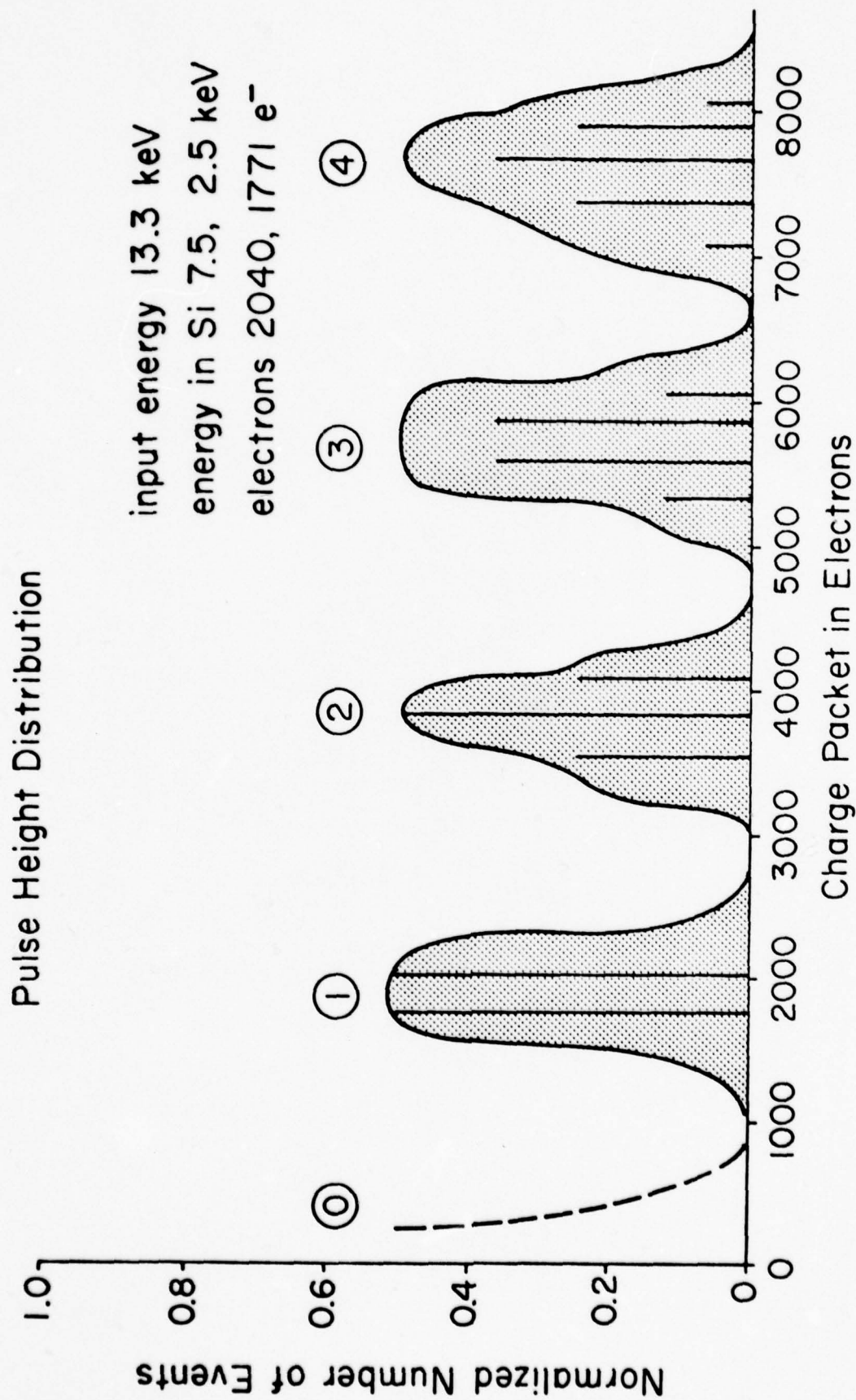


FIGURE 2

## V. Advantages of Single Photoelectron Discrimination

In this section we distinguish between single photoelectron sensitivity and single photoelectron discrimination in a photodetector. In a conventional photomultiplier, this distinction is the difference between operating in an analog or "DC" mode and operating with a discriminator set to trigger at the single photoelectron level. In order to illustrate this distinction more clearly for a television or scanning system, several parameters will now be defined. The nominal CCD-201 has a saturation level of 75 millivolts which is equivalent to  $0.4 \times 10^6$  electrons. Under the operating conditions similar to those discussed in the previous section, a single photoelectron will produce a charge packet of 2,000 electrons. We presume for the sake of discussion that the thermal leakage charge and the thermal leakage noise are zero. Let us now consider the dynamic range and the noise level for such a detector system. The maximum number of photoelectrons per pixel per scan is thus 200. If the "random noise" has a value which is larger than 2,000 electrons, then the dynamic range is linearly related to the noise level. This is illustrated in the left hand portion of Figure 3 where the dynamic range is determined by the ratio of the random noise level and the saturation level. The dotted line extends this relation for lower noise levels. However, as the noise level decreases we have the option of a different type of detection based upon the discrete character of the photoelectron. Thus we may introduce the discriminator and operate in a mode in which, intuitively, the discriminator will never be tripped when there are no photoelectrons. The dynamic range would then be infinite. However, from a more practical point of view, a finite noise distribution has a "tail" so there are occasional times when the discriminator is actuated, producing an "electronic dark current". However, the value of the electronic dark current or the probability of tripping this discriminator decreases far more rapidly than linearly with a decreasingly

## Relation Between Dynamic Range and Single Photoelectron Discrimination

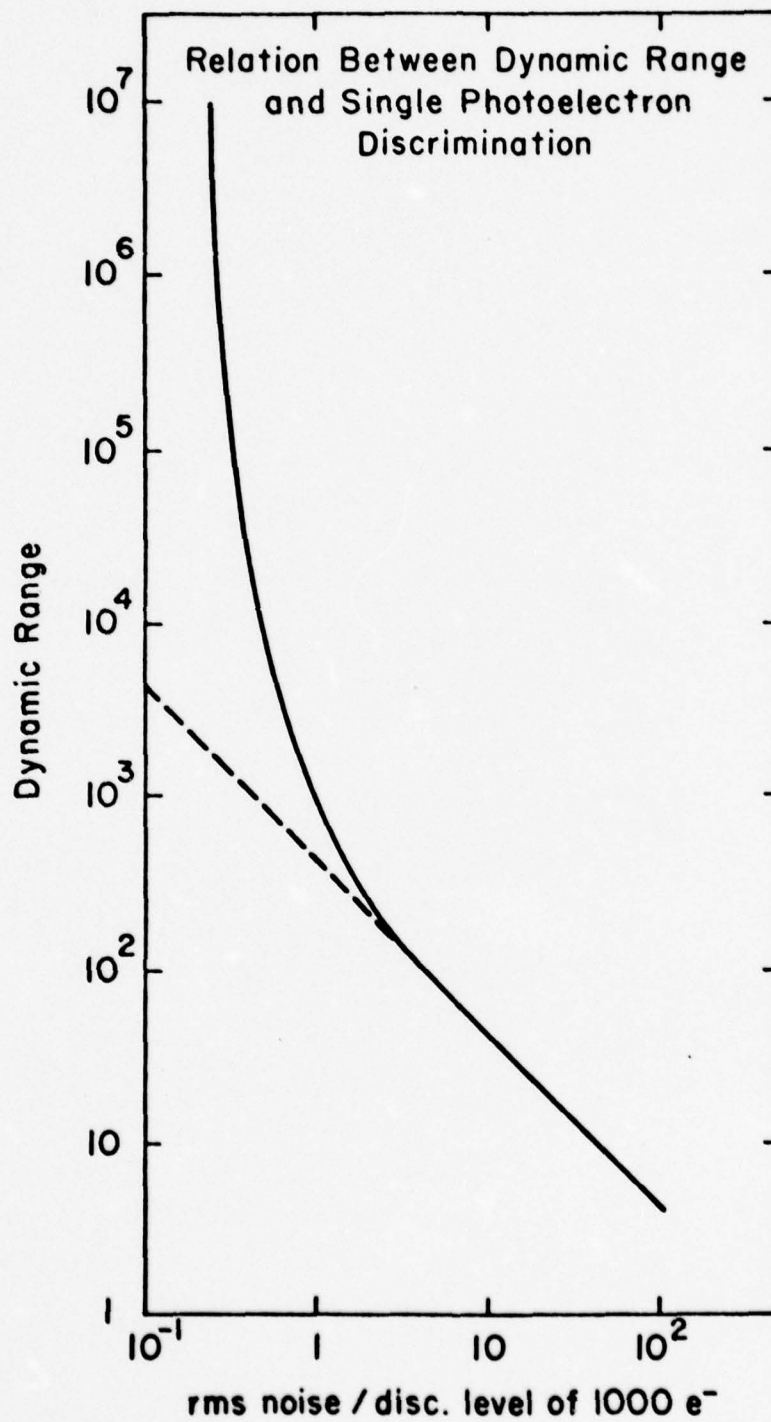


FIGURE 3



noise level. Thus if the discriminator is set equal to 1,000 electrons and the random noise has a value of 1,000 electrons (giving an effective collection efficiency of 84%), the probability of tripping the discriminator by the noise in each pixel in a given scan is about 0.16 so the dynamic range is about 1300. If the random noise level is one half as large (500 electrons), then collection efficiency is 98% and the probability of tripping the discriminator is about 2.3%. Thus the dynamic range is increased by a factor of seven to 2,000,000. This general relation is indicated in the left hand portion of Figure 3 which presumes Gaussian statistics for the random noise. Thus we see the critical importance of decreasing the noise and operating in a single photoelectron discrimination mode, since small reduction in random noise increases the dynamic range by several orders of magnitude rather than by proportional factors.

## VI. Saturation, Blooming and Lag

In this section we briefly mention several problems which normally affect scanning sensors.

### A. Saturation

Saturation is defined as the departure from a linear relation between input light intensity and output electrical signal. For the moment, we ignore the processes analogous to the computer processing methods which are used to get "linear" results from film by unfolding an H-D curve. The single photoelectron discriminator curve which relates input to output has a break point at one photoelectron per pixel per scan. Actually, for normal MAAI operation, this break point occurs at three photoelectrons per pixel per scan. This value then parameterizes the Single Photoelectron Discrimination (SPD) saturation. However, if a parallel analog channel is used, the break point for the "analog saturation", is defined by using the nominal 75 millivolt saturation of the CCD-201. For the parameters of the earlier section, this occurs at about two hundred photoelectrons per scan per pixel.

### B. Blooming

The term "blooming" is used in this discussion to describe the appearance of apparent photo response in pixels which receive no light, but are located near pixels which are receiving illumination. There are three types of blooming:

Radial Bloom is normally seen in conventional low light level devices. It is caused by various mechanisms including the electron beam spread. Due to internal structures in the silicon and the lack of an electron beam, there is almost no radial bloom in the CCD.

Vertical Bloom occurs due to spilling of charge from an overloaded photosite into the transfer register location which are "passing by". This occurs at an illumination beyond the analog saturation level, which, in turn, is well beyond the normal operating levels for single photoelectron discrimination.

Horizontal Bloom occurs primarily due to a lower transfer efficiency for the horizontal transfer registers operating at 4 MHz. This type of blooming occurs as apparent light in one horizontal line only. Existing data may be used to place an upper limit on the magnitude of this effect. It will produce excess light in a horizontal line which is fainter than the "diffraction spikes" which occur due to the spider in a reflecting astronomical telescope.

C. Lag

Lag describes the residual charge left at a photosite from the previous frame. This is not significant below saturation and above saturation should be small, but has not yet been measured.

## VII. Damage Mechanisms

When a CCD is bombarded on the front surface by photoelectrons with an energy of 10 to 20 KeV, there may be radiation damage which interferes with proper semi-conductor operation. While there are a variety of different damage mechanisms, proper operating conditions and some of the special properties of the CCD-201 will prevent a number of these problems. The mechanism which remains most important is related to the effect of holes left in the  $\text{SiO}_2$  when the photoelectron causes ionization in the insulating layers. General radiation damage measurements which have been conducted at the Naval Research Laboratory<sup>5</sup> indicate that this type of damage will result in a significant operational lifetime problem. the actual lifetime will depend upon details of operating procedures and conditions. Several further techniques are now being investigated for extending the operating life of the ICCD. One of these techniques consists of increasing the thickness of the aluminum protection. This is one aspect of reducing, as much as possible, the amount of ionization in the critical layers. In addition, there are several procedures that have shown promise in annealing or removing the damage. These techniques have been successful in other types of devices but have not been properly tested on the CCD-201.



#### VIII. Test System Description

The basic description of the Single Scan Data System is illustrated in the block diagram of Figure 4. The voltage sequences which are required to drive the CCD are developed in the Video Driver Unit. This is a separate rack mounted unit. In addition to the high impedance pulse trains, this unit also develops the required voltages for driving the CCD. Clock drivers within the camera mount, on the video drive board, convert the high impedance pulse train into the high current pulse trains required for the CCD. The actual performance of the CCD, as well as a detailed description of the electronic system will appear in a separate report.

In the Mark II Camera Head (Upgraded), the video output from the CCD is processed in a separate chamber which is electrically isolated from the chamber in which "scanning" pulse currents are generated. This video processor card contains a preamplifier, a sample and hold amplifier which is gated from the Video Driver Unit, a second amplifier, and a DC restoration circuit.

The output of the video processor card may be amplified and used for a direct CRT display, using special outputs from the Video Driver Unit to provide the proper voltages to form a raster.

The video signal from the video processor card then proceeds to an Input/Output card in the NOVA 2/10 computer. Here the signal is again sampled and converted from analog to digital form. A special multiplexing circuit then compacts the 8-bit or 4-bit data from the A/D converter into 16-bit NOVA words. This permits the use of the NOVA direct memory data rate of 1.2 MHz for 16-bit words or a CCD data rate of 4.8 MHz with 4-bit digitization (2.4 MHz for 8-bit digitization).

Block Diagram of Single Scan Data System for Evaluation of ICCD

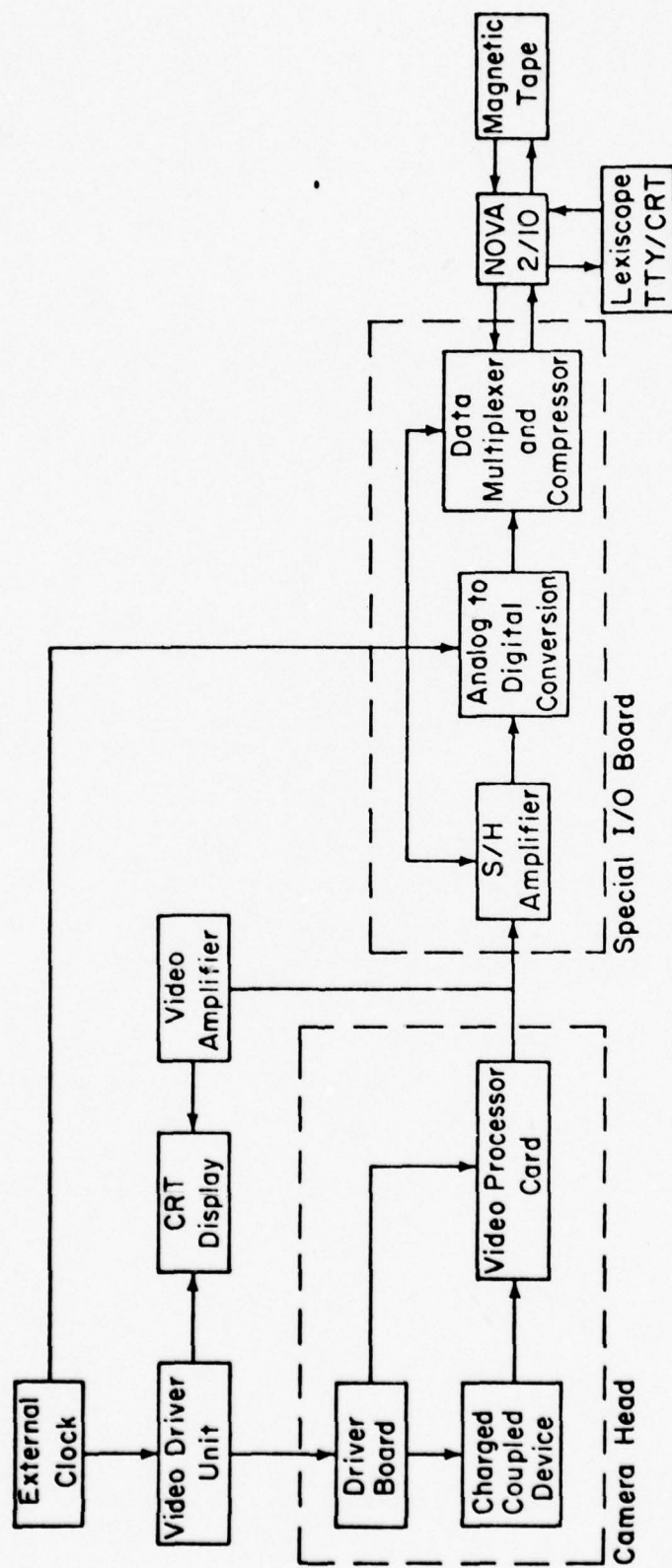


FIGURE 4

The control of the NOVA, which includes the storage and selection of the array data, is handled by a Lexiscope CRT terminal. While this data is stored in the NOVA 2/10 core, one can command, with the Lexiscope terminal, a bar chart display of a single line in the array. This permits the inspection of the data within the NOVA core prior to recording on magnetic tape. Following this inspection, on command from the Lexiscope, the data is transferred from NOVA core to the Precision Instruments magnetic tape unit for recording on 9-track magnetic tape.

The magnetic tape is then read by a special program written for the UNIVAC 1108 which unpacks the NOVA words into FORTRAN readable 36-bit words and/or writes these pictures into an Image Processing System picture format file. The arrays of data are then processed by the Image Processing System (IPS) which has been written for the Amplitude Interferometry Program. The output for the IPS system employs several of the I/O devices of the Computer Science Center, in particular, teletype display, CRT display, line printer output, or the Computer Science Center digital optical scanner. The Image Processing System will be described in more detail in separate publications.

The entire Single Scan Data System is rack mounted in special shipping containers to permit convenient field operation.

## IX. Operating Data System

For normal operation of the ICCD on a telescope, there are several additional requirements placed on the data processing system. Since we expect to operate the ICCD at a data rate of 4 MHz, this will require some method of data storage and successive frame addition which has a cycle time of 350 nanoseconds. In order to satisfy the requirements for the MAAL application, a Circulating Semi-conductor Memory (CSM) has been fabricated. This unit has five independent tracks, each of which has an ultimate capacity of 12, 288 words containing 16-bits. The data is entered through five arithmetic units which are presently programmed to either add the new data word to the existing word, or to produce a zero. However, the arithmetic unit has the capability of being programmed for a total of 32 logical operations on their two inputs. The data which is circulating in the CSM may be removed on data bus. The data buses from each of the five tracks are multiplexed to a common data bus. This common data bus is connected to the NOVA 2/10 minicomputer core by the direct memory access mode. Thus the data can be transferred directly from the CSM to the NOVA 2/10.

In this mode, the CSM is serving as a temporary, high speed, storage device. However, it serves another purpose. By placing a "skeleton" of control words in the CSM and certain logic and control functions in the hardware, the CSM controls, in detail, the voltages used in scanning of the CCD. In this mode, the CSM controls the horizontal and vertical scanning and inserts the data words between the control words in the CSM. Since this "skeleton" is entered to the CSM via a program contained in the NOVA 2/10, one may enter special skeletons to cause special scanning modes (i.e. scanning a small rectangle in the CCD array). These control modes are defined by interjecting a new control skeleton into the CSM from the NOVA 2/10. The CSM has been completed and presently is operating in stand alone mode. The interface to the mini-computer has been completed and is being



tested. With a modification in a control card, the CSM can also do real time subtraction of sky background.

### References

1. Choisser, J. P., Experiments on the Use of CCD's to Detect Photo-electron Images, paper presented at Symposium on Charge Coupled Device Technology for Scientific Imaging Application, Jet Propulsion Laboratory, March 1975.
2. D. G. Currie, ON A DETECTION SCHEME FOR AN AMPLITUDE INTERFEROMETER NAS-NRC Woods Hole Summer Study on Synthetic Aperture Optics 1968.
3. D. G. Currie, ON THE ATMOSPHERIC PROPERTIES AFFECTING AN AMPLITUDE INTERFEROMETER NAS-NRC Woods Hole Summer Study on Synthetic Aperture Optics, 1968.
4. D. G. Currie, S. L. Knapp, and K. M. Liewer, FOUR STELLAR-DIAMETER MEASUREMENTS BY A NEW TECHNIQUE: AMPLITUDE INTERFEROMETRY, The Astrophysical Journal, Vol. 187, No. 1, Part 1, January 1974.
5. R. H. Dyke and M. D. Jack; LOW LIGHT LEVEL PERFORMANCE OF THE CCD-201 (an unpublished report from the Fairchild Corporation).
6. J. M. Killiany, W. D. Baker, N. S. Seks, and D. F. Barbe, EFFECTS OF IONIZING RADIATION ON CHARGED COUPLED DEVICE STRUCTURE: IMEE Transactions on Nuclear Science, Vol. NS-21, December 1974, p. 193.

APPENDIX IV

AN INTENSIFIED CHARGE COUPLED DEVICE  
FOR EXTREMELY LOW LIGHT LEVEL OPERATION

AN INTENSIFIED CHARGE COUPLED DEVICE  
FOR EXTREMELY LOW LIGHT LEVEL OPERATION

Douglas G. Currie  
Department of Physics & Astronomy  
University of Maryland

The theory of operation and operating data on the Intensified Charge Coupled Device (ICCD) which is being developed within the Amplitude Interferometry Program at the University of Maryland will be discussed. The ICCD is an electro-optical system which is, in effect, a very high sensitivity "television camera system" converting a two dimensional image into serial video data. This system uses a modification of the standard Fairchild CCD201 incorporated in a vacuum tube with electrostatic focusing. The Electronic Vision Company of San Diego has fabricated the vacuum tube, which uses a photocathode that has been externally processed by molecular beam techniques. Each photoelectron produced at the photocathode is accelerated to about 15 Kev. On impact upon the front side of the CCD, the photoelectron produces extensive ionization in the active silicon and thus a charge packet at the photosite. This charge packet is sufficiently large, compared to all the various noise sources, to permit a clear discrimination between no photoelectron and one photoelectron. Thus the video processing system will then provide a discrete digital signal for each photoelectron. Such a system can yield an extremely large dynamic range.

In order to reduce the thermal leakage noise, the CCD within the tube is cooled to  $-20^{\circ}\text{C}$  by a circulating fluid-dry ice cooler. The electronic noise sources in the ICCD and the mechanisms of the background noise level will be discussed to show the special advantage of using single photoelectron discrimination to obtain very large dynamic range. A dynamic range



of more than one thousand has already been obtained for the CCD operation and this is sufficient to obtain for a very large (more than 30,000) dynamic range in the photoelectron counting ICCD mode. The electronics system which provides the array scanning voltages and the video signal processing, with the proper sensitivity and stability for field operation, is incorporated in the Single Scan Data System. This Single Scan Data System operates the CCD and the array scanning, processes the video data, records the data in temporary storage for display and verification, and then records the data on 9-track magnetic tape.

The magnitude of the charge packet produced by the ionization has been determined as a function of acceleration voltage between 10 KV and 18 KV. The results of these measurements and of electron penetration of the transfer gate protection (when the tube is operated above the operating value of 15 KV) will be discussed. Data on the detection of single photoelectron pulses will also be presented.

The mechanism and magnitude of saturation, blooming and lag, as they occur in the ICCD, will be discussed. Preliminary measurements of those parameters, using the Single Scan Data System on the CCD and the ICCD, will be presented. The various damage mechanisms which are due to bombarding the CCD with the accelerated photoelectrons, and the resultant limits on the operating lifetime of the tube will be discussed. Measurements relating to the operational lifetime will be presented.

The primary objective of this work on the ICCD is to provide a sensor for a specialized instrument which yields diffraction limited imaging on large aperture telescopes. For use in this Multi-Aperture Amplitude Interferometer application, the data must be processed and recorded in real time at the video rate. For this purpose, a high speed, five track memory which

operates at 5 MHz has been designed and fabricated. This Circulating Semi-conductor Memory (CSM) has a storage capacity of 12,288 words of 16 bits for each of the five tracks. The CSM is now in operation and the entire data system of which this is a part, will be described.

## APPENDIX IV

A PHOTON COUNTING ARRAY PHOTOMETER USING  
AN INTENSIFIED CHARGE COUPLED DEVICE

A PHOTON COUNTING ARRAY PHOTOMETER USING  
AN INTENSIFIED CHARGE COUPLED DEVICE

Douglas G. Currie

Technical Report # 77-037

PP # 77-128

December 1976

Presented at IAU Symposium # 40

University of Paris

7 September 1976



# A PHOTON COUNTING ARRAY PHOTOMETER USING AN INTENSIFIED CHARGE COUPLED DEVICE

DOUGLAS G. CURRIE

University of Maryland, College Park, Maryland USA

## ABSTRACT

An array photometer which uses an Intensified Charge Coupled Device has been developed at the University of Maryland. This system, the University of Maryland Array Photometer (UMAP) has the ability to discriminate single photoelectron events in real-time at a 4 Megahertz rate. The photosensor uses an S-20 photocathode and a Fairchild CCD202 with a 100 by 100 array of separate individual channels. This is an electrostatically focused device fabricated by the Electronic Vision Company. The overall system has demonstrated a noise level which permits single photoelectron discrimination, a scan rate of 400 frames per second, a very linear response, and very low lag. The UMAP system has a very large dynamic range exceeding 10,000 in the photon counting mode. A special technique to extend the dynamic range to 1,000,000 will be described. The performance parameters of this system, both in the laboratory and on the telescope will be discussed. It has already been operated in the photon counting mode on several different telescopes. Data from these observations will be discussed to illustrate the system sensitivity (which is at a level defined by the photocathode sensitivity and the spacial resolution), which is basically limited by the pixel size in the array, rather than the electro-optics.

## I. Introduction

The University of Maryland Array Photometer consists of an array of photo-sensitive channels, each of which is capable of single photoelectron discrimination, or photon counting. This system, in its basic form, is not saturated by a uniform illumination of 400 photoelectrons per pixel per second, i.e., a photoelectron rate of  $4 \times 10^6$  photoelectrons per second for the entire array. The photodetector of this system is an internally Intensified Charged Coupled Device fabricated by the Electronic Vision Company and built around a Fairchild CCD201/202. Several of these Intensified Charge Coupled Devices (ICCD) have been fabricated by the Electronic Vision Company (a division of Science Applications, Inc.) and tested at the University of Maryland. These tests have been conducted primarily using the Single Scan Data Recording System with some preliminary tests conducted using the full University of Maryland Array Photometer system.

## General Properties of the Array Photometer

The University of Maryland Array Photometer (UMAP) system, using an ICCD, is an ultra-sensitive TV-type camera system which distinguishes individual photoelectrons in each of 10,000 channels. These channels are arranged in the form of an array of one hundred by one hundred elements. The time resolution in each channel is normally somewhat shorter than three milliseconds, which is the time required to scan one frame. The frame time, and thus the time resolution, may be much smaller if a shorter subarray is scanned. The array is sensitive to the incident light for essentially all of the observational period (i.e., greater than 98% of the time) and the expected dynamic range for each channel in the basic system is very large, about 250,000 for a ten minute observation. For the extended (analog) system, this expected dynamic range is  $5 \times 10^7$ .

### Internally Intensified Charge Coupled Device

The basic photodetector for the University of Maryland Array Photometer (UMAP<sup>®</sup>) system is the Intensified Charge Coupled Device (ICCD). In this device, an incident photon is converted to a photoelectron at the photocathode. In the current tubes, the photocathode has response similar to the S-20 response. The photoelectron is accelerated and focused, and then penetrates the region of active silicon in the Charge Coupled Device, where ionization produces a charge packet. The scanning circuitry of the CCD provides the parallel-to-serial conversion of the data, and the video signal is preamplified by circuitry on the CCD substrate.

### History and Current Status

The development of the UMAP electronics and of the Single Scan Data Recording System (SSDRS) was started late in 1973. A preliminary set of electron bombardment tests of a CCD were performed at the Electronic Vision Company in August of 1974 using the preliminary form of the SSDRS. The initial contract for tube fabrication from the University of Maryland to the Electronic Vision Company was let in October of 1974. ICCD-1 was received for testing at the University of Maryland in June of 1975. This tube proved to be gassy after an initial series of tests were completed. ICCD-3 was received at the University of Maryland in September of 1975, and has shown no problems with gas. ICCD-4 was received in February of 1976. The results of earlier tests have already been reported <sup>(1)</sup>, and this report will primarily focus on the results obtained with ICCD-3.

The overall system is currently operating at a noise level which permits single photoelectron discrimination and permits the formation of images with discriminated single photoelectrons. The system has been operated in this fashion on a variety of astronomical telescopes. Although the UMAP system is not yet in full operation, and the results are quite preliminary, the various aspects of the system which have been carefully tested are in accord with the early theoretical predictions. <sup>(2)</sup>

## II. Requirements for the Array Photometer

The development effort described in this report has been motivated by two different applications at the University of Maryland. These applications, although they are both astrophysical in nature, generate a significantly different set of requirements on the array photometer.

### Amplitude Interferometer Requirements

The primary application of the UMAP system is to provide the basic photo-sensor for a new astronomical instrument, the Multi-Aperture Amplitude Interferometer (MAAI). This unique new system is a multi-channel version of the Amplitude Interferometer which has been used in an astronomical observation program over the last four years <sup>(3,4,5,6,7)</sup>. When used on a large telescope, the current instrument yields image information, through the earth's atmosphere, which has a resolution that is somewhat better than the diffraction limit of the telescope. The MAAI will have an angular resolution which is about the same as the currently operating instrument of i.e., 0.010 arc-seconds when used on the 200-inch telescope on Palomar Mountain. The precision of the measurements which have been made with the current instrument are about 0.002

arc-seconds (7). This will be greatly improved with the new MAAI, which has a data rate which is larger by a factor of about 7,000 and which utilizes all of the light received by the telescope primary.

Basically, the MAAI application requires an array of individual photosensors, each of which has:

1. The ability to discriminate reliably among zero, one, two, and more than two photoelectrons per pixel per scan,
2. Very low lag, i.e., very little memory from one frame to the next frame,
3. Minimal cross talk between spacial channels (or pixels) and high geometric stability.

The requirements on the overall array are:

1. At least 100 by 100 elements,
2. The ability to complete the scan of a full frame in a few milliseconds, and subframes at a rate of much faster than the basic 400 frames a second.

#### Direct Imaging Camera Requirements

The other application in which the Array Photometer will be used consists of a Direct Imaging Camera in the focal plane of a large telescope. Although initially planned for use on an earth-based telescope in conjunction with the MAAI, the low weight, the electrostatic focusing, and low power requirement of the system make it very interesting for space applications. For one, most of the above requirements are important, but the imaging application has the additional requirements of:

1. Very large dynamic range,
2. Very low blooming.

Some of the electronic operating parameters of the system will be significantly different when the UMAP system is used in these two different applications.

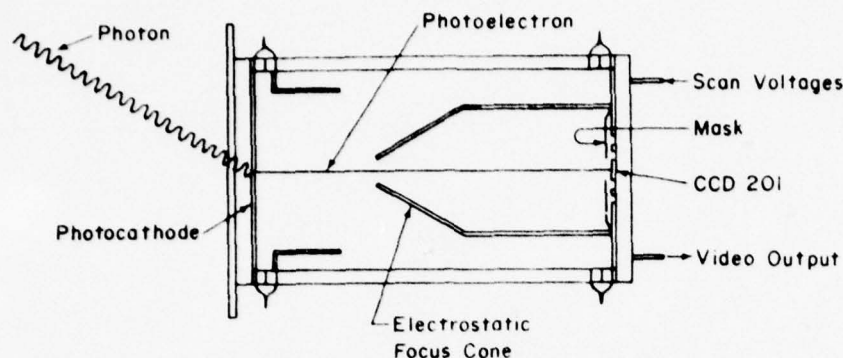
### III. Method of ICCD Operation

In this section, we briefly describe the theory of operation and the detailed design of the ICCD. Both of these areas have been previously described in more detail in the literature (2,8).

#### Theory of Operation of the ICCD

The incident photons are received on a semi-transparent photocathode, where they are converted into photoelectrons. On the current devices, this is an S-20 photocathode. As indicated in Figure 1, these photoelectrons are accelerated to an energy of about 15 Kev and electrostatically focused onto the front surface of a Fairchild Charge Coupled Device (CCD201, or the current and future ICCD's, the CCD202).





Schematic Diagram of Intensified Charge Coupled Device  
Figure 1

The photoelectron penetrates the overlying layers of circuitry (where some energy is lost) and creates a packet of charge at one of the photosites by ionization of the silicon. This accumulation of individual packets of charge created by separate photoelectrons may continue until the end of the integration cycle. The charge packets which have accumulated during the integrating cycle (which is typically a few milliseconds) is then moved from the photosites to the transfer registers. The period during which the charge is transferred from the photosites to the shift registers is about 50 microseconds. During this period (about 2% of the integration cycle) the system is insensitive to light. The transfer registers move the charge line by line vertically from the two-dimensional array of photosensitive sites to the horizontal transfer register. Here one performs a parallel-to-serial conversion. The charge packets then go to the on-chip preamplifier. These transfer registers operate independently of the photosites and at the same time that the photosites are integrating the electrons produced by ionization for the next frame. Thus the transfers or "scanning" take place during the integration period, and the array is sensitive more than 98% of the time.

The transfer registers are protected by a layer of aluminum on the front surface of the CCD and the accelerating voltage is chosen so that those bombarding electrons which fall on the transfer sites do not reach the active silicon. Thus when operating in the direct imaging mode one loses a factor of two in effective quantum efficiency. The protection of the aluminum means that one does not have any ionization or "interline noise" in the transfer registers.

Electrical Operation of the CCD The scanning of the CCD is controlled by a set of control words in the Circulating Semiconductor Memory which will also store the data. In order to operate the light sensor on the telescope, a long cable from the electronics to the camera head is required. To handle this, a special camera head has been fabricated which minimizes the cross-talk and coherent noise. The pulse trains are transmitted to the telescope on high impedance lines. These are converted to the required high current pulses by clock drivers in the camera head. The camera head also contains amplifiers, a sample and hold circuit, and a discriminator.



Noise Sources in the Charged Coupled Devices There are three types of electronic noises which are most significant with respect to ideal photoelectron discrimination operation. These effects which will be defined in the following paragraphs are "random charge noise", "thermal leakage charge" and the variation of the thermal leakage current or the "thermal leakage noise".

The random noise is the variation of the voltage level, from one frame to the next, at a given pixel. For measurements of the random noise, the illumination is presumed to be constant, or as for most of these tests, there is no illumination. The random noise is characterized by the standard deviation of the voltage at a given pixel for a number of successive frames. This type of noise behaves as if it were Johnson noise dominated by the capacitive input of the on-chip preamplifier. The value of the random noise is essentially independent of temperature (more precisely it varies inversely as the absolute temperature). At a data rate of 0.5 MHz the random noise has been measured by Dyck and Jack<sup>4</sup> to be about 300 electrons per pixel per scan. We find about the same value at 0.5 MHz and about 1.0 MHz.

The "dark current" or thermal leakage current is due to thermally generated charge pairs which are created within the active silicon. The leakage current is parameterized by the average number of electrons which collect at a given pixel during the integration interval (usually this is equal to the scan or frame time). The value of the thermal leakage charge varies across the frame from pixel to pixel. It decreases by a factor of two when the temperature of the CCD is reduced by 6 or 7°C and decreases linearly as the integration time is decreased. The average leakage charge across the frame does not significantly effect the ICCD operation but its variation across the chip may create a problem. The variation of the thermal leakage charge from frame to frame (Poisson Statistics) in the leakage electrons would properly be a component of the random noise, but its value is negligible for normal ICCD operation.

The "thermal leakage noise" or fixed pattern noise is the variation of the thermal leakage charge across the array. This will be parameterized by the standard deviation of the thermal leakage charge across the array. More precisely, it is the variation of the mean (over many frames) thermal leakage charge across the array. This latter form of the definition removes the random noise as a component of the thermal leakage noise. It should decrease with temperature at the same rate as the thermal leakage charge and decrease in proportion to the increased data rates. This has been verified as will be discussed later. In order to permit single photoelectron discrimination without a change of discriminator level for each pixel, this fixed pattern noise must be reduced to about 100 electrons. Although this should be satisfied at room temperature, it may safely be accomplished by cooling to approximately -20°C.

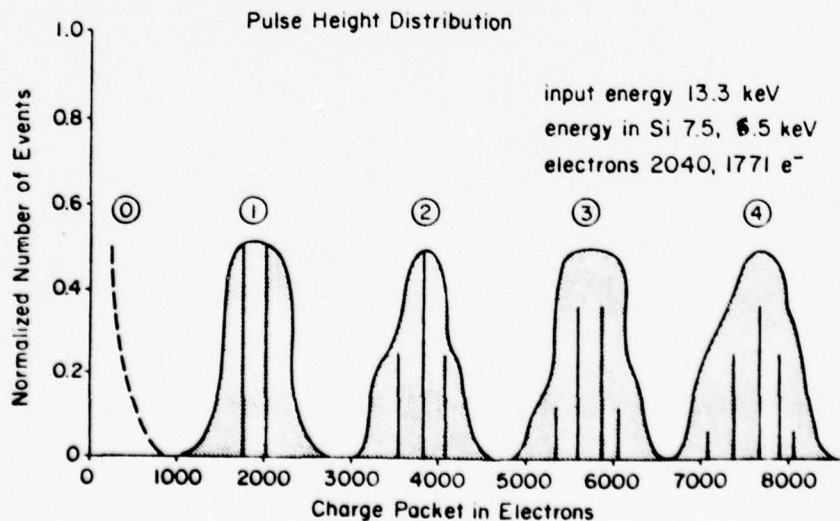
In order to study these quantities, an Image Processing System has been developed at the University of Maryland which permits computer processing of many scanned frames and the determination of these quantities by a standard procedure.

#### Operation of Intensified CCD

In this section we discuss the intensification of the CCD201 in more detail.

Theory of Intensification The photoelectrons provided at the photocathode are accelerated to 14.6 KeV prior to impact on the CCD. This value will provide sufficient charge by ionization to permit the detection of a single photoelectron, but is not sufficient to penetrate the aluminum (and other layers) which form the protection for the transfer registers. Since different regions covering the transfer registers have different thicknesses, the accelerating voltage is chosen so the photoelectron cannot penetrate the thinnest region. For a photoelectron which impacts the CCD over a photosite, some of the energy is lost in the layers of silicon and silicon dioxide which lies over the photosite. The 14.6 KeV electron will encounter either of two regions over the photosites which have different thicknesses. Therefore, the photoelectron may have either 8.5 or 9.6 KeV upon entry to the active silicon. These detailed calculations are based on a specific model of the CCD architecture which was obtained from R. Dyck of the Fairchild Corporation. For any given device from a particular run, it is expected that there will be significant variations. Thus these numbers may be considered as a sample calculation.

As a result of the energy of the photoelectron entering the active silicon, we will have the production of charge packets containing 2300 or 2600 electrons, depending on how many layers it has penetrated. The variation of these numbers is relatively small, especially when compared to noise in the on-chip amplifier of 300 electrons. Since the incident electrons may enter either area, we expect an ideal pulse height distribution of the electrons to have the form indicated by the vertical bars in Figure 2. For this case, the energy has been further reduced to 13.3 KeV so the photoelectron will not penetrate into the final layers of  $\text{SiO}_2$  insulation above the active silicon of the transfer registers. The cross-hatched area represents the pulse height spectra for the case in which the noise of the on-chip preamplifier is included. The different values depend upon the energy of the accelerated electron, i.e., the accelerating voltage.



Thus, for an incident energy of 13.3 KeV, and depending upon what region of the photosite the electron enters, a packet of either 1,770 or 2,040 ionization electrons is produced for each photoelectron. Since the noise in the on-chip preamplifier is about 300 electrons, one may easily discriminate between a single photoelectron or no photoelectrons.

#### ICCD Design

The design of the ICCD incorporates several features which enhance the ability to discriminate at the single photoelectron level. A special CCD201, on which most of the top layer of  $\text{SiO}_2$  (the scratch protection) was not added, was mounted by the Fairchild Corporation on a ceramic header. This header, designed by the Electronic Vision Company, provides the required electrical contacts for the CCD in a circular pattern of pins. Thus it may be mounted in a socket in the camera head which was developed for the ICCD. The header also provides the support for the electrostatic focus cone and the mask which exposes the active array and protects the preamplifier and other circuitry on the chip from damage by the accelerated photoelectrons. The chip is bonded directly to the ceramic header so the CCD may be readily cooled using a probe which contacts the header directly below the CCD. This is an area which is clear of pins. The cooling may be required to reduce the thermally generated dark current on the chip.

#### IV. University of Maryland Array Photometer System

Since the UMAP system described in this section has been developed primarily as the photosensor for the Multi-Aperture Amplitude Interferometer, several aspects of the system are especially oriented toward this goal. In particular, there are several requirements on the system beyond those general requirements discussed in Section II which are related to operation at the Cassegrain or prime focus of a large telescope. These are:

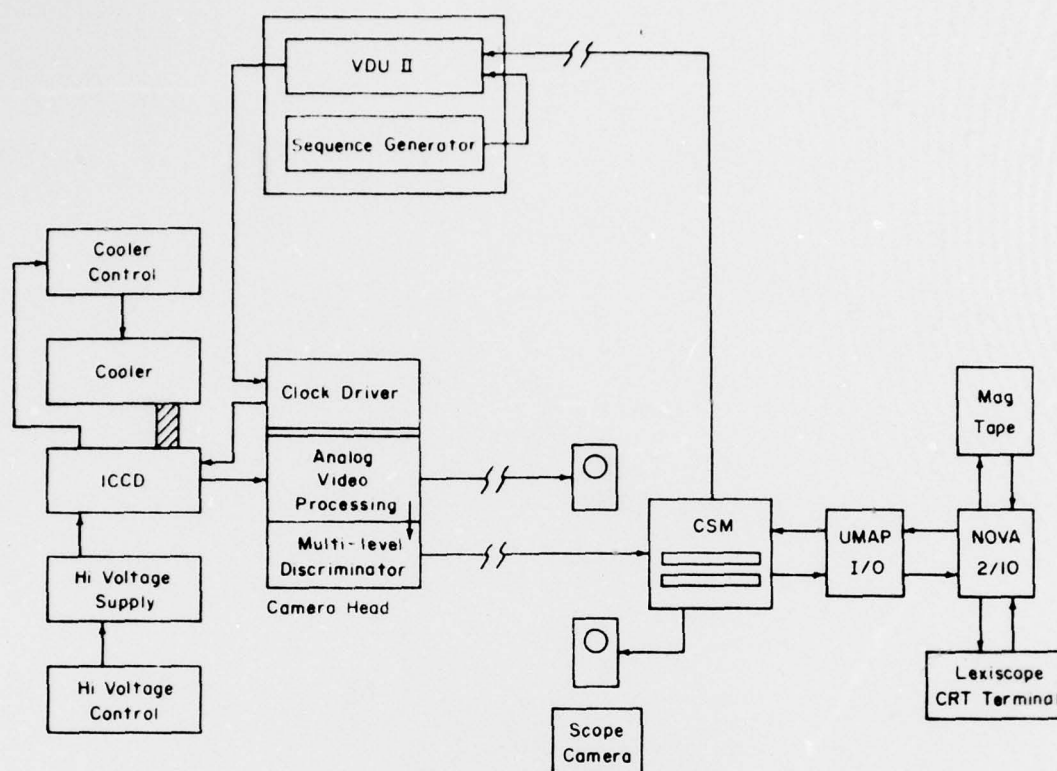
1. Operation over a wide temperature range,
2. Photometer unit which is light weight, mechanically and optically rugged, and operable at all orientations.
3. High immunity to external RFI,
4. Proper operation with main electronics subsystems located 100 meters from photometer unit, i.e.,
  - a. a minimum of cross talk between the signals transmitted on the cable
  - b. proper sequencing of the various clocks in order to handle propagation delays which consist of several cycles,
5. Equipment packaging to permit the use of air freight in an "assembled" configuration.

The following discussion will center on the use of the ICCD as the photosensor for the UMAP system. However, the UMAP system is also designed to use bare CCD's as infrared sensors with a few minor additions. The use of the UMAP system within the MAAI involves a rather complex overall system. Thus to simplify the following discussion, we shall describe the use of the UMAP system with the Direct Imaging Camera. This will use part of the MAAI system, but the additional capabilities and complications involved in the MAAI system will be either ignored or mentioned only in passing in this discussion.

#### Block Diagram of UMAP System

The block diagram of the University of Maryland Array Photometer system, as it will be used in the "Direct Imaging Camera" mode, is shown in Figure 2.





Block Diagram of UMAP System as Used in the Direct Imaging Camera Mode

Figure 3

We shall now proceed to describe the overall operation of the UMAP system. Depending on the particular requirements of the observations, the scan rate, the format and the size of the array to be scanned is chosen by the operator. The parameters which describe this subarray are typed into the lexiscope CRT interface. The NOVA mini-computer then generates the detailed instructions which are required for scanning the CCD in this particular fashion. The NOVA cannot operate at the speed required to directly control the CCD, so these commands are transferred and stored as special control words in the Circulating Semiconductor Memory. The Circulating Semiconductor Memory (CSM) is a special memory device which has been designed and fabricated for this application. It has five tracks (only one of which is used in the Direct Imaging Camera mode) each containing 12,288 words. The individual words are 16-bits deep. The total memory capacity of the CSM is 0.6 M bits and it currently operates with an input of 5, 3-bit words at a rate of 75 M bits per second. The CSM, which operates at a data rate as high as five megahertz, transmits these individual commands to the Video Drive Unit (VDU) which is located on the telescope near the photometer unit. The Video Driver Unit generates coded pulses to drive the CCD. The CCD may be cooled by a thermoelectric device to reduce the variations of the dark current across the chip to a value which is small compared to the random capacitive input noise on the on-chip preamplifier. This temperature is typically between 20°C and -20°C. The video output from the CCD, which contains the data, is brought to an electrically isolated portion of the camera head, i.e., separate from the chamber which contains the CCD drive circuitry. This configuration reduces the pick-up of coherent noise by the sensitive video electronics. The video signal is amplified and the signal divided for the two types of processing. On the one hand, the charge from each photosite is discriminated at various preset voltage levels for use in a photon-counting mode. On the other hand, an A/D conversion



is performed on the other portion of the signal. This permits the operation of the CCD in a linear or analog; rather than photon counting mode. The information, in digital form is transmitted from the telescope down to the Video Processing Unit. The Video Processing Unit has a very simple function for the Direct Imaging Camera. However, in the MAAI, it performs the on-line computations which are required to transfer the data into a structure in which one may add successive frames of data. From the Video Processing Unit, the data stream proceeds to the Circulating Semiconductor Memory, where this data is added, pixel by pixel, to the data of the previous scans. Thus one channel of the CSM records data at a five Megahertz rate for a three bit word. For all five channels the CSM accepts data at a rate of 75 megabits/sec and records them in a memory which totals 0.6 Megabits of storage. One may select, either by thumb wheel or by software, various different sizes of memory and various different rates of operation. For permanent storage of the data, the NOVA minicomputer slows down the CSM in a predetermined sequence, transfers a block of data from the CSM to the NOVA core storage, sets the registers in this block in the CSM to zero, and accelerates the CSM to the proper rate and reinitializes the CCD. The data is then transferred from the NOVA core storage to digital magnetic tape while new data from the CCD is being recorded in the CSM.

#### Projected System Performance of UMAP System

Let us now consider the predicted performance of the overall system. The intrinsic dynamic range for the UMAP system is extremely large (i.e. of the order of  $5 \times 10^7$  per pixel for a ten minute integration). Since the overall system is not yet operating at this level, these predictions will be based on data from several sources, some of which will be discussed in later sections.

Operational Direct Imaging Performance In most applications, practical aspects of the application will prevent the use of such a large dynamic range. For example, when the system is used to record the direct images of faint objects with a wide spectral range on a large telescope, the effective dynamic range is defined by various parameters of the overall UMAP/telescope system and of the atmosphere. Thus to make a realistic projection for a given observational situation, we will consider the overall configuration which was to be used for quasar observations on the 200-inch telescope at Palomar Mountain in January of 1976. The photometer unit was installed at the prime focus, with Ross corrector lens system, and a set of spectral filters. However, to achieve the maximum performance in terms of the high dynamic range, none of these optics would be used. For the photocathode response, we use the measured quantum efficiency of the "S-20" photocathode of ICCD-1. For this illustrative calculation, we shall express the results in units of the image brightness expressed in stellar magnitudes per square arc-second. Thus we primarily address the study of an extended object, like a distant galaxy. We note, however, that if the seeing disk is slightly larger than one arc-second, the ordinate and abscissa of Figure 4 may also be correctly interpreted in terms of the visual magnitude of an unresolved source. Thus this analysis permits a condensed presentation to both the observation of a quasi-stellar or unresolved object (expressed in stellar magnitudes) and to an extended object (i.e., a faint galaxy) where the surface brightness is expressed in stellar magnitudes per arc-second. A more complete discussion, including the dependence of this performance on the diameter of the seeing disk will be presented elsewhere.

Dynamic Range Extension by Use of Analog Mode There is no blooming until at least several hundred photoelectrons per pixel per scan are accumulated. Thus if we were to record data on the SSDRS at the same time as the photon counting data is recorded in the CSM, we would obtain an additional factor of, conservatively, 200 in the dynamic range. The current camera heads permit this but the improvements required for the rest of the equipment have not yet been implemented. Thus we see from the figure that the dynamic range for this configuration is 16.4 stellar magnitudes or about  $3.5 \times 10^6$ .

Thus this mode of operation includes the use of the data from regions bright enough to require operation in the analog region of the CCD. For this analog measurement, we have presumed that the limit in the accuracy of the measurement may not be the photon counting statistics, but the accuracy to which the systematic problems may be corrected. For the solid line in Figure 3, we have presumed that the systematic errors can be corrected to a level at which we have already found that we can perform this correction during some early tests at the University of Maryland (i.e. 0.3%). The dotted line indicates a correction at a level of 0.05%, which has been achieved during more recent tests. We note that Fairchild has published data claiming this may be corrected to a level of 0.025%.

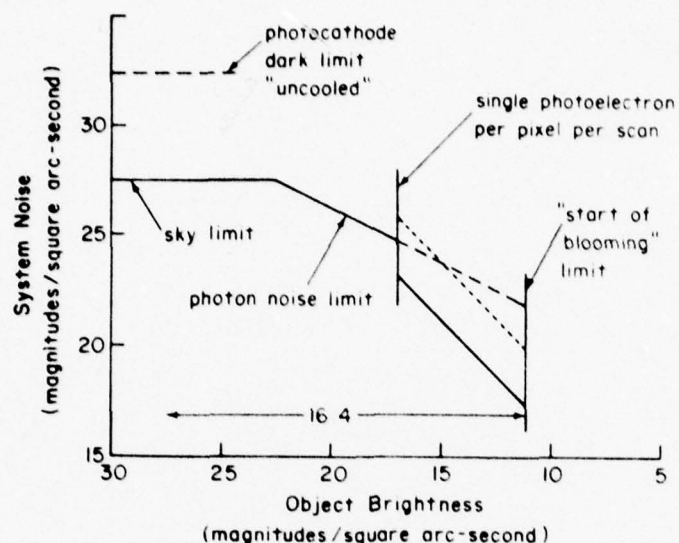
This projected performance makes the UMAP system particularly interesting for use in observing objects which have a very large dynamic range over a relatively small field. Since the response of each individual pixel is independent at this signal level, one can expect operation here with very little blooming. For the configuration of the telescope and the UMAP system described in this section, the effect of the insensitive aluminum transfer registers on the photometric accuracy for observing unresolved objects is less than 0.05%. We are particularly interested in the study of Seyfert galaxy cores and quasars, with a determination of the type of the underlying galaxies in the latter case.

Assumptions for Limiting Performance. In the operation mentioned, the limiting magnitude is defined by the statistical noise in the night sky background. However, in the absence of the night sky, there are two effects which will limit the ultimate dynamic range. The first of these is the emission of thermal electrons from the photocathode in the absence of light (photocathode dark current) and the other is caused by large random noise excursions tripping the discriminator (electronic dark current).

The theoretical evaluation of the expected level of the electronic dark rate makes several assumptions.

1. The "random noise"<sup>(2)</sup> of the CCD has a standard deviation of 300 electrons,
2. The distribution of this random noise is indeed Gaussian to the required level. Preliminary data on this point will be discussed in a later section of this paper.
3. The chip architecture, and the resultant pulse height distribution have the form which has been described earlier <sup>(2)</sup>,
4. The discriminator operating point is set at a level of .320 electrons to yield a collection efficiency of 93%.

This results in a limiting magnitude due to electronic dark current (in the 1-T sense) of  $m_v = 32.4$  for a ten minute exposure.



Limiting system noise of UMAP system, where the abscissa describes the surface brightness expressed in magnitudes per square arc-second and the ordinate describes the equivalent brightness of the "noise" or uncertainty in an observation of a pixel expressed in stellar magnitudes.

Figure 4

In general, the figure describes the observation of an extended area for which the brightness of this object may be, for example, 20 magnitudes per square arc-second. In this case, the "system noise" will be about 26 magnitudes per arc-second, or it will have a standard deviation (if several observations of ten minutes are taken) of 0.4% which, in this domain, is due to the Poisson noise of the signal. Thus we might expect to see, at a "one-sigma" level, a feature with a brightness of 26 magnitudes per square arc-second overlying a region with a uniform brightness of 20 magnitudes per square arc-second.

For an object with a brightness between 16.9 and 22.5, this uncertainty in the intensity of the image (the "system noise") is due to the Poisson counting statistics in the signal from the object. This is based upon an assumed observation interval of ten minutes. This also assumes a visual brightness for the moon-less night sky at Palomar Mountain of 22.5 magnitudes/square arc-second. For objects fainter than 22.5 magnitudes, the dominant noise source is the Poisson statistics in the night sky. In the range from 16.9 to 11.2, the noise may be either Poisson or systematic as will be discussed in more detail later. We have presumed an "uncooled" photocathode. The plate scale is about 11"/mm, giving a field of 33" by 44". The UMAP system will discriminate among zero, one, two, and more photoelectrons <sup>(2)</sup>. Thus one may have a mean count rather close to the frame rate of 400 frames a second, and still have a reasonably small correction for four and more counts. We shall nominally assume a mean rate of 400 photoelectrons per second per pixel for the maximum rate which is still in the single photon counting rate. For the faint limit of the dynamic range, we obtain a brightness of 27.5 magnitudes which is equal to the statistical Poisson noise in the night sky, i.e., we have here a signal-to-noise ratio of one. Remaining in the photon counting mode, we then have a dynamic range of 10.6 magnitudes or 17,400.



The 'uncooled' dark current limit presumes that the system is operating at about 'observatory' temperature of 50°F which we have found to be representative of the dome temperature. This calculation is based upon dark current rates which we have observed in the field and at the University of Maryland on similar devices with S-20 surfaces. This is in accord with published S-20 data.<sup>(8)</sup> One then obtains a limiting magnitude of 32.2, or about one photoelectron in ten minutes which is indicated in Figure 3. The addition of a procedure for cooling the photocathode would reduce this noise source, but this is not particularly effective, since then the electronic dark noise would immediately dominate.

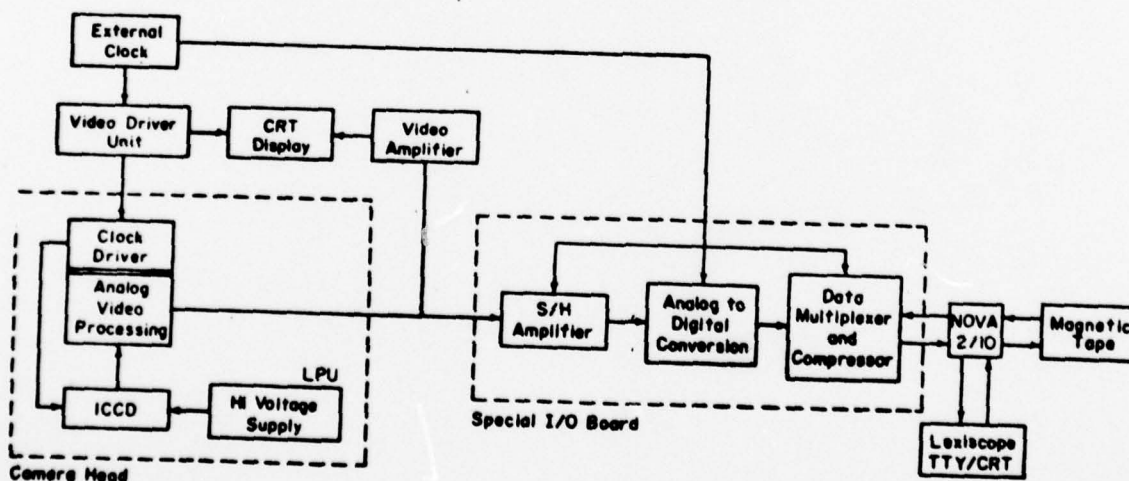
For applications in which one is not limited by sky noise (i.e., imaging with narrow spectral filters or for spectrophotometry), we would have a photon counting range of  $6.3 \times 10^5$  and a total dynamic range of  $1.3 \times 10^8$ . However, the computations of these theoretical results are extremely sensitive to the assumption made on the electronic dark current.

## VI. Laboratory Performance

In this section we consider various tests and evaluations which have been conducted in the laboratory.

### Single Scan Data Recording System

In order to evaluate the performance of the various portions of the system prior to the full operation of the electronics of the UMAP system, a test system, the Single Scan Data Recording System<sup>(9)</sup> (SSDRS) was designed, fabricated, and put in operation in May of 1974. A block diagram of the SSDRS is shown in Figure 5.



Block Diagram of the Single Scan Data Recording System  
Figure 5



The basic mode of operation is to perform an A/D conversion for each pixel at a data rate which may be as high as four megahertz. A single frame of data words is then stored in the NOVA core. This stored frame of data is written onto digital magnetic tape. The rate at which frames may be recorded is limited by the magnetic tape writing speed to about three frames per second. Most of the laboratory and telescope data has been collected with this system. In several cases there appears to be some noise pickup which may dominate the effects of the noise in the CCD and in the camera head. In addition, we have recently discovered a one pixel shift in the recording of the data which has led to an apparent increase in the noise. Recent measurements, after fixing the jitter, on ICCD-4 which has a CCD202, indicate a random noise of about 300 electrons.

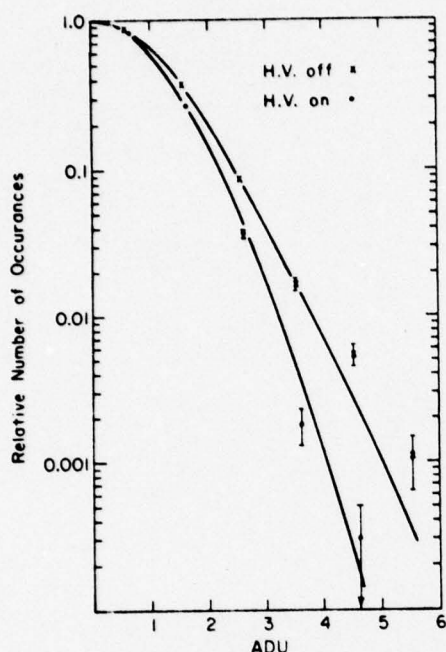
#### CCD System Noise Level

In this section we consider effects of "noise" which would degrade the system performance. The first of these effects to be considered here is the "random noise", followed by a consideration of the "fixed pattern noise".

We now consider the apparent random noise which one observes at the CCD. This has been measured in various laboratories including our own, to have a typical value of about 300 electrons.

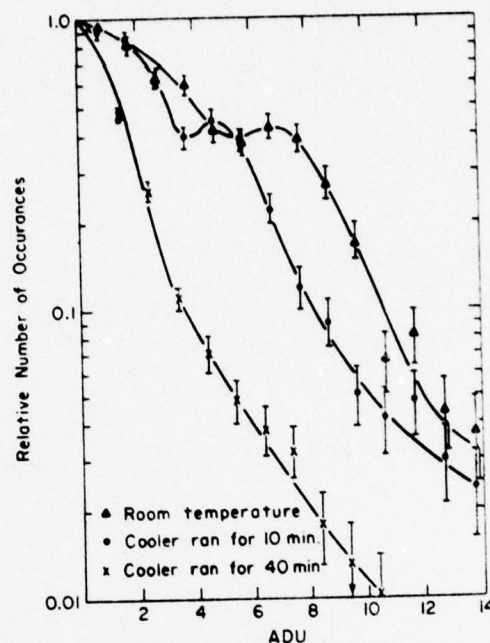
In order to evaluate our data for this purpose, we shall use a pulse height distribution over many elements of the array. The pulse height distributions are formed by the following sequence of operations. One first records ten frames from the CCD with no illumination falling on the CCD or the photocathode (a "dark frame"). These are then averaged. Ten frames are then recorded during which the photocathode is illuminated (an "illuminated" frame). One then subtracts from a single illuminated frame, pixel by pixel, the averaged dark frame, and then performs a pulse height analysis of the remaining array. Usually this pulse height analysis is done over a central subarray, to reduce computer costs and to eliminate edge effects. The pulse height analysis consists of forming a pulse height distribution, i.e., the number of times one observes a given sized pulse or a given voltage for a pixel as a function of the pulse height or the voltage on the pixel. This analysis is repeated for each of the ten frames and the ten pulse height distributions which are produced are summed to produce a total pulse height distribution. This may be displayed directly (as seen in Figure 8) or we may normalize the peak of the pulse height distribution to unity and plot the upper side of this curve, which is relevant to photoelectron discrimination, as seen in Figure 6.

The random noise of the CCD is indicated in Figure 6 and is seen to be about 1.1 A/D Converter Units (ADU). The effect of turning on the high voltage is indicated by the pulse height distribution denoted with o. The difference is not significant, since differences of this magnitude occur for runs separated by an interval of time. As indicated above, more recent tests have demonstrated a standard deviation of 300 electrons.



Pulse Height Distribution of Random Noise for ICCD-3. The ADU are each 0.124 millivolts at the CCD.

Figure 6



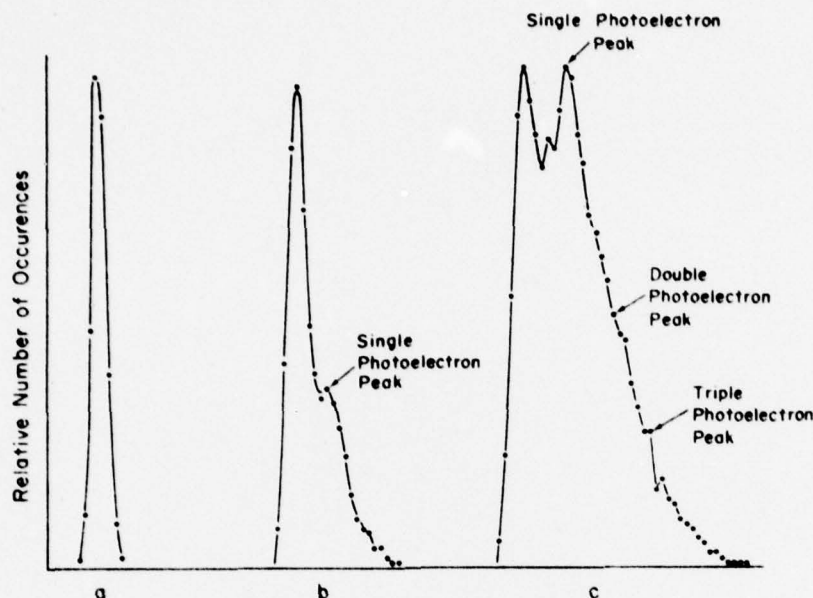
Pulse Height Distributions of Thermal Leakage at Three Different Temperatures.

Figure 7

The other source of noise is the "fixed pattern noise" or the spacial variations of the thermal leakage current in the silicon. The two types of noise are independent and combined in a simple manner, so they may be studied separately. The fixed pattern noise is then evaluated by averaging ten frames (to reduce the effect of random noise). A pulse height distribution is then obtained for the values expressed in the averaged frame. At room temperature and at a scan rate of 0.5 MHz, these variations in dark current are expressed in Figure 7 and are unacceptably large. The variation becomes much smaller and quite acceptable as the CCD is cooled. On the other hand, when the CCD is operated at 4 MHz, the width of the peak should be reduced by another factor of eight, which also makes the width quite acceptable.

#### Single Photoelectron Pulse Height Distribution

We now wish to evaluate the magnitude of the signal from a single photoelectron. In order to do this, the photocathode is illuminated with a uniform intensity and the recorded data is used to obtain the single photoelectron pulse height distribution. This has been done with various voltages and various light intensities. Three of these pulse height distributions are indicated in Figure 8.



Pulse height distribution with 15 KV, 15 KV, and 18 KV, respectively and with no illumination, illumination, and illumination respectively.

Figure 8

Figure 8a illustrates the random noise of the CCD with no light input. This shows a relatively narrow peak with a standard deviation of 1.2 ADU. In Figure 8b, the photocathode is uniformly illuminated with an accelerating voltage of 15 KV. The peak due to the single photoelectrons can be seen. The peak due to zero photoelectrons is somewhat enlarged to about 1.5 ADU, and the mean magnitude of the single photoelectron signal is 5.3 ADU. In Figure 8c, where the accelerating voltage has been increased to 18 KV, the zero photoelectron peak is further broadened to about 2.0 ADU. This may be due to some penetration occurring at this (above nominal) accelerating voltage. The position of the single photoelectron peak (with respect to the ICCD photoelectron peak) is 7.5 ADU. Finally, the width of the single photoelectron peak is 3.0 ADU. In order to compare these values with the predictions, we must determine the gain of the on-chip preamplifier. The nominal value <sup>(10)</sup> is 1.5 Volts/picocoulombs, however, this may have wide variations <sup>(10)</sup>. Thus to determine the value for this present chip, we use the change in accelerating voltage and the change in peak position. This implies  $380e^-/\text{ADU}$  or the gain of 2.0 Volts/picocoulomb, and implies the measured signal at 14.4 KV (which was calculated in an earlier work <sup>(2)</sup>) would be  $1780e^-$  compared with the theoretical value of  $1910e^-$ , well within the accuracy of this determination and knowledge of the various layers on the chip surface. The additional width of the singles peak is also in agreement with predictions <sup>(2)</sup>. That is, in Figure 8c, the singles peak is 1.0 ADU wider than the zero photoelectron peak and the prediction is that the additional width is 0.7 ADU.

The behavior of an individual channel or pixel in the ICCD is comparable to the performance of a conventional photomultiplier. Using the data expressed in Figure 8c, and setting the discriminator at a level to obtain a collection efficiency of 84%, one has a dark current rate of one count per second, which is a rather respectable performance, even at this preliminary stage.



### Spacial Resolution

The spacial resolution of the electrostatically focused ICCD-3 was evaluated, using a microprojector to place a small spot of light ( $\sim 7\mu\text{m}$ ) on the photocathode. In the central region (out to a radius of about 1.3 mm in the 3mm by 4mm format), essentially all of the light fell within a single picture element. In this region, the diameter of the electron image of the incident light was less than 20 micrometers. This was determined by moving the incident light spot until the electron image fell on the aluminum transfer register between two photosites which has a width of 20 micrometers. No response was seen in either of the adjoining photosites where the sensitivity of this determination was at least 10% of the peak response. Thus in this region, the MTF of the UMAP system is basically the MTF of an array of discrete pixels. However, around the outer edge of the array the electron image spread to cover more than a single pixel.

### VII. Field Operation

Operational tests using the Single Scan Data Recording System with the bare CCD's and the ICCD's have now been conducted on a variety of telescopes. The purpose of these tests have been to:

1. evaluate the field problems (low temperatures, transportation, "fool-proof operation")
2. determine the sensitivity of the system to external interference (TV and FM)
3. evaluate the system sensitivity

Some of these tests were conducted on the 36-inch telescope (which is operated by the Laboratory for Optical Astronomy) and the 48-inch telescope (operated by the Laser Technology Branch). Both of these groups are within the Goddard Space Flight Center and the telescopes are located at the Goddard Optical Research Facility (GORF). In addition, the photometer system was operated at the 60-inch and 100-inch telescopes at Mt. Wilson, and preliminary tests were also conducted on the 200-inch telescope at Palomar Mountain, which are operated by the Hale Observatories. A detailed list of these observations appears in Table I.

### Field Configuration of System

The system configuration which has been used in these tests consists of the Single Scan Data Recording System. Although the CCD has not been cooled, the ambient temperature has ranged, on various observational runs, between  $0^{\circ}\text{C}$  and  $20^{\circ}\text{C}$ . A number of different objects have been observed in order to calibrate the sensitivity and to evaluate the general performance.



TELESCOPE	FOCUS	DATE	OBJECT	PHOTO- SENSOR	PLATE SCALE ARC-SEC/PIXEL	COMMENTS
100-inch Mt. Wilson	Cassegrain	8 July 1975	$\epsilon$ Her, etc.	CCD	$0''.178$	System operation Test of TVI sensitivity
Mt. Wilson	50 mm lens**	7 July 1975	Antares	CCD	$146''$	Sensitivity test & camera calibration
60-inch Mt. Wilson	50 mm lens	19 July 1975	Jupiter	CCD	$146''$	System operation Test of TVI sensitivity
36-inch GORF*	135 mm lens	24 Oct. 1975	Jupiter	ICCD-3	$54''$	Determination of the system QE
Sorrento Valley **	135 mm lens		Pleiades	ICCD-3	$54''$	Blooming and resolution measured
48-inch GORF	Coude	November 1975	$\alpha$ UMa	ICCD-3	$0''.197$	Determination of the system QE
36-inch GORF	Cassegrain	16 Nov. 1975	Jupiter, $\gamma$ Ari, 30 Tau, Landolt 095-0206	ICCD-3	$'' .56$	Determination of the system QE
36-inch GORF	Cassegrain		Landolt 095-0206	ICCD-3	$'' .56$	System Sensitivity
36-inch GORF	Cassegrain	19 Nov. 1975	30 Ari, Saturn Trapezium	ICCD-3	$'' .56$	Evaluation of imaging
			Saturn		$1''.00$	Evaluation of imaging
100-inch Mt. Wilson	Cassegrain	28-31 Dec. 1975	$\zeta$ UMa, $\alpha$ Per, 14 Aur, 39 Leo	ICCD-3	$0''.178$	Star calibration of sensitivity and effects on TVI determined.
200-inch Palomar Mtn.	Prime Focus	8-10 Jan. 1976	Star	(ICCD-3)	$0''.39$	†

\* Goddard Optical Research Facility, Beltsville, Maryland

\*\* 50 mm lens and 135 mm lens are camera lenses

†† Electronic Vision Co., Sorrento Valley, San Diego, California

† Due to power supply accident no observations performed with ICCD, however, some observations were made with a simulated ICCD. Alignment and operational procedures developed.

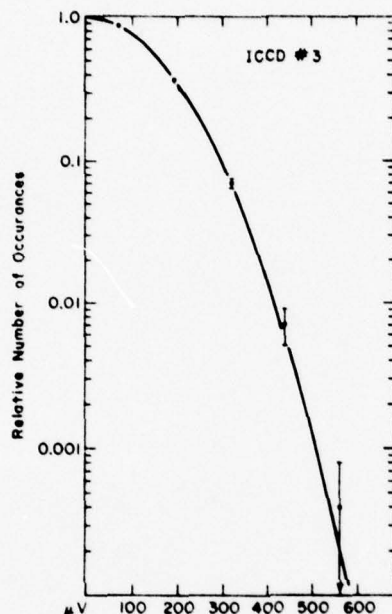
Table I  
Operation of UMAP System on Astronomical Telescopes

### Telescope Mounting of Photometer Unit

The photometer unit (which is about 4" by 5" by 6") was mounted in a different fashion at each of the telescopes. On the 36-inch telescope at GORF, this was mounted at the Cassegrain focus by means of an existing adapter, a 4" by 5" holder. The operation using the 48-inch telescope at GORF was at the Coude focus and the photometer unit was tripod mounted within the Coude room. The mounting on the 100-inch telescope was at an auxiliary focus at the Naismith Cassegrain position. This was formed with a bending mirror attached to the Amplitude Interferometry Mounting Adapter. The mounting on the 200-inch was at the prime focus using the Westphal bracket for the SIT camera while the Amplitude Interferometer was mounted at the Cassegrain focus. This dual configuration permitted rapid change over between the two instruments (approximately 15 minutes).

### Results of Telescope Operation

We first consider Figure 9, which shows the random noise when the system is operated on the telescope at the Goddard Space Flight Center.



Pulse Height Distribution of Random Noise  
Measured on 36-inch Telescope at GORF  
Figure 9

For the calculation of the dynamic range, it was assumed that the statistical behavior of the random noise was Gaussian over 4.5 orders of magnitude. In Figure 9, the Gaussian curve, fitted to the three highest points, is indicated by the solid line. Although this data does not cover the full range of five decades, this data is Gaussian, within the statistical error bars of the measurement. Even at Mt. Wilson, where 30 Megawatts of TV and FM power are emitted within one mile of the dome, and where the analog signal sent along 150 feet of cable, the apparent random noise was not excessive and the monitor display was quite acceptable. This apparent random noise due to external pickup should not be a problem when the discrimination is done within the camera head.

### System Performance

We now discuss the results which were achieved with the SSDRS operating on the various telescopes. The general purpose of the stellar observations has been to calibrate the sensitivity of the system. As indicated in the table, the stellar observations have been conducted on the 36-inch, the 48-inch, and the 100-inch telescopes. Generally, these tests have indicated a system response within a factor of two or three of the predicted system response. A more precise comparison is difficult, since the quantum efficiency of the photocathode dropped by a factor of ten from the values measured during tube fabrication (about 20% at peak) to the values measured at the end of the tests. The reason for this decrease is being investigated. However, the system seems to behave as predicted using the value of the quantum efficiency measured

after the test. This assumes the loss was due to an event early in the tube lifetime. In addition to the stellar images, direct images of several objects were recorded. In particular, Saturn was observed with a neutral density filter to reduce the intensity by 100. This resulted in a multi-photoelectron signal per pixel per scan. The set of four stars which compose the Trapezium was observed with neutral density filters which reduced the light level by factors of 10 and 100. The first set of data has about ten photoelectrons per pixel per scan, while the second set of data on the Trapezium had about one photoelectron per pixel per scan, at the brightest region.

The Trapezium data was then discriminated in the computer. That is, the dark frames were averaged and subtracted from each frame with the image on it. Then each time a pixel had a signal as large as one photoelectron, a total frame was incremented by one unit. This "software discrimination" was applied to a set of 100 frames of data, and yielded a reasonable image of the configuration. During exposure to normal (low) light intensity, there has been no obvious cumulative damage to the CCD by the accelerated electrons, either due to a lack of damage inflicted or due to self-annealing between exposures. When the tube (ICCD-3) was exposed to high levels of light, there has been obvious increases in dark current which have apparently not self-annealed. Similar affects due to high level illumination have already been reported<sup>(1)</sup>. However, these regions of increased dark current become negligible in magnitude when the CCD is cooled.

#### Conclusions

An array photometer using an ICCD as the photodetector has been designed, developed, and fabricated. It is currently being tested in the laboratory and on the telescope. The performance in the tests up to this time has been generally in accord with predictions.<sup>(2)</sup> The system has performed imaging on the telescope with discriminated single photoelectrons. The ICCD has operated reliably in the laboratory and in the field for five months. A test of the full system is expected shortly.

#### Acknowledgements

Many people and groups have aided this effort. We very much appreciate the generous amounts of telescope time which have been made available by the Hale Observatories and by the Goddard Space Flight Center, both for the ICCD work, and for the Amplitude Interferometry. At the University of Maryland

I would especially like to thank Robert Braunstein, who has been responsible for the major effort in obtaining the operating data on the UMAP system and analyzing this data. The electronics of both the UMAP system and the SSDRS has been brought into reality by John Giganti and the Electronics Shop at the University of Maryland. Most of the development and programming of the NOVA and Eclipse system has been done by Al Buennagel. The programming and rather extensive computations which have been required for the data analysis have been performed by S. Kaisler, A. Blumenthal, and L. Bleau of our group. This was done on the UNIVAC 1108 of the University of Maryland Computer Science Center which is supported in part by NASA Grant NGR 398. I would also like to thank John Choisser, Jim McPherson and Peter Bertling for their work on the ICCD at Electronic Vision Company.

Various different aspects of the work on tube fabrication and system development have been supported by grants and contracts to the University of Maryland from the National Science Foundation (MPS-74-05890-001), National Aeronautics and Space Administration (NGR-21-002-444), Office of Naval Research (N00014-75-C-0343), and to Science Applications, Inc. from USAF Space and Missile Systems Organization (FO4701-75-C-0068).



### References

1. D. G. Currie, AN INTENSIFIED CHARGE COUPLED DEVICE FOR EXTREMELY LOW LIGHT LEVEL OPERATION, presented at the 1975 International Conference on the Application of Charge Coupled Devices, sponsored by the Naval Electronics Laboratory Center, 29 October 1975.
2. D. G. Currie, ON A PHOTON COUNTING ARRAY USING THE FAIRCHILD CCD201, presented at the symposium on Charge Coupled Device Technology for Scientific Imaging Applications, 6 March 1975, p. 80, JPL SP 43-21. This appears in somewhat extended form in University of Maryland Technical Report # 75-082.
3. D. G. Currie, ON A DETECTION SCHEME FOR AN AMPLITUDE INTERFEROMETER NAS-NRC, Woods Hole Summer Study on Synthetic Aperture Optics, Vol. II, p. 35, 1968.
4. D. G. Currie, ON THE ATMOSPHERIC PROPERTIES AFFECTING AN AMPLITUDE INTERFEROMETER, NAS-NRC Woods Hole Summer Study on Synthetic Aperture Optics, Vol. II, p. 79, 1968.
5. D. G. Currie, S. L. Knapp, and K. M. Liewer, FOUR STELLAR-DIAMETER MEASUREMENTS BY A NEW TECHNIQUE: AMPLITUDE INTERFEROMETRY, the Astrophysical Journal, Vol. 187, p. 1 January 1974.
6. S. L. Knapp, D. G. Currie, and K. M. Liewer, ON THE EFFECTIVE TEMPERATURE OF  $\alpha$  HERCULIS A, Astrophysical Journal V 198, 561, 1975, University of Maryland Technical Report # 75-006, July 1974.
7. Stellar Disk Diameter Measurements by Amplitude Interferometry, 1972 - 1976, Currie, Knapp, Liewer and Braunstein, Technical Report # 76-125, submitted to Astrophysical Journal.
8. J. P. Choisser, EXPERIMENTS ON THE USE OF CCD'S TO DETECT PHOTOELECTRON IMAGES, presented at Symposium on Charge Coupled Device Technology for Scientific Imaging Applications, 6 March 1975, p. 150, JPL SP 43-21.
9. LARGE SPACE TELESCOPE, PHASE A, FINAL REPORT.
10. L. A. Buennagel, D. G. Currie, R. Braunstein, A PRELIMINARY DESCRIPTION OF THE SINGLE SCAN DATA RECORDING SYSTEM, University of Maryland Technical Report # 76-038.
11. R. H. Dyck, private communication.